



Cite this: DOI: 10.1039/d5pm00315f

## Graphene oxide in antibiotic delivery and synergistic antibacterial action

Mark Dakurah,<sup>†a</sup> Hasibul Islam,<sup>†a</sup> Khandoker Asiqur Rahaman,<sup>b</sup> Nadeem Baig<sup>c</sup> and Shihab Uddin<sup>\*,a,b</sup>

The rise of antibiotic-resistant bacteria has created an urgency to develop advanced antibiotic delivery systems. Nanoscience can address this issue by providing nanocarriers that enhance efficiency and minimize side effects in antibiotic delivery. Nanoparticle-based delivery systems can mechanistically combat antibiotic resistance by improving intracellular antibiotic delivery and antibiotic concentrations, protecting antibiotics from enzymatic degradation, increasing penetration into bacterial biofilms, and targeting antibiotics, unlike conventional antibacterial strategies, which lack these capabilities. An ideal antibiotic nanocarrier, therefore, requires a high antibiotic-loading capacity, controlled and stimuli-responsive release, intrinsic antibacterial activity, biocompatibility, and surface functionalization for targeted delivery. Graphene Oxide (GO) meets all these criteria due to its unique physicochemical properties. It has emerged as a promising antibiotic nanocarrier that offers high drug-loading capacity, tunable surface chemistry, and multifunctional antibacterial mechanisms. However, its performance is strongly dependent on dose, lateral size, oxidation degree, and surface functionalization, leading to inconsistent reports on efficacy, toxicity, and translational feasibility. This review describes GO's prominent role in antibiotic delivery and its synergistic action with antibiotics to combat antibiotic-resistant bacterial strains, while critically analyzing the mechanistic interactions between GO and antibiotics, the variability in reported biological outcomes, and the limitations of existing studies. Finally, key trends and unresolved controversies, including GO-antibiotic synergy and antagonism, and translational challenges related to stability, toxicity, and scalability, are critically discussed to guide future research on prospects of GO in antibiotic delivery against multidrug-resistant bacteria and define realistic pathways toward pharmaceutical and clinical development.

Received 4th November 2025,  
Accepted 16th May 2026

DOI: 10.1039/d5pm00315f

rsc.li/RSCPharma

### 1. Introduction

The global health concern of antibiotic resistance is one of the leading threats in the twenty-first century. It is currently a major concern due to the growing number of antibiotic-resistant bacteria attributed to the excessive and improper use of antibiotics, as well as the slow rate of antibiotic discovery. More alarmingly, it has been predicted by the World Health Organization (WHO) that around 10 million annual deaths will occur by 2050 without effective countermeasures.<sup>1</sup> Thus, antibiotic resistance has been recognized as an urgent challenge to public health by the WHO, as antibiotic-resistant bacteria

expose the weaknesses of conventional antimicrobial treatments.<sup>2</sup> As bacteria develop key survival mechanisms, including antibiotic-modifying enzymes, changes in membrane permeability through porins and efflux pumps, and modifications to the antibiotic-binding site to reduce intracellular antibiotic concentrations and drug-target interactions,<sup>3</sup> combination antibiotic therapies, which were the best choice solutions, are rendered ineffective, as indicated by the literature.<sup>4</sup> Thus, many clinically dangerous bacterial strains are developing antibiotic and multidrug resistance, rendering treatment with conventional drugs ineffective. Moreover, some antibiotic-resistant bacteria can transfer the antibiotic-resistant gene to other bacteria through horizontal gene transfer, thereby increasing the number of antibiotic-resistant bacteria and making traditional therapies ineffective.<sup>5</sup> Thus, resistant bacteria are developing faster than the discovery of new antibiotics. This exacerbates the situation and presents a challenge in the treatment of antibiotic-resistant bacteria, thereby necessitating the development of innovative methods.

In this regard, nanoparticle-based antibiotic delivery systems have emerged as a viable option for mechanistically

<sup>a</sup>Department of Bioengineering, King Fahd University of Petroleum & Minerals, 31261 Dhahran, Saudi Arabia. E-mail: shihab.uddin@kfupm.edu.sa; Tel: +966138605564

<sup>b</sup>Interdisciplinary Research Center for Bio Systems & Machines, King Fahd University of Petroleum and Minerals, Dhahran 31261, Saudi Arabia

<sup>c</sup>Interdisciplinary Research Center for Membranes and Water Security, King Fahd University of Petroleum and Minerals, Dhahran 31261, Saudi Arabia

<sup>†</sup>Both authors contributed equally.



combating antimicrobial resistance rather than just replacing current antibiotics because they have the potential to increase intracellular antibiotic accumulation, protect antibiotics from enzymatic degradation, improve penetration into bacterial biofilms, and promote targeted interactions with bacterial membranes, thereby overcoming key resistance mechanisms like efflux, reduced permeability, and enzymatic inactivation.<sup>6,7</sup> Nanomaterials possess several properties relevant to the fight against multidrug-resistant microbes, including intrinsic antibacterial activity through biofilm penetration, microbial membrane damage, oxidative stress, and physicochemical interactions that disrupt bacterial metabolic and structural integrity.<sup>8</sup> However, an ideal antibiotic nanocarrier should possess high antibiotic loading efficiency, controlled and stimuli-responsive release, stability under physiological conditions, and minimal host cytotoxicity, while maintaining predictable pharmacokinetics and acceptable biodistribution profiles.<sup>9</sup> Among the diverse nanocarrier platforms investigated, nanomaterials that combine intrinsic antibacterial activity with antibiotic-delivery properties are particularly attractive, as they can function as both carriers and active antimicrobial agents. Thus, GO stands out as a revolutionary candidate due to its exceptional properties as a nanocarrier, as it is often described as biocompatible and low in toxicity at lower concentration ranges, chemically versatile, with a high surface area, and exhibits antibacterial activity through membrane disruption, wrapping of bacterial cells, and oxidative stress.<sup>10</sup> Nevertheless, these biological effects are highly dependent on GO concentration, lateral size, oxidation degree, and surface functionalization, leading to significant variability across reported studies.<sup>11</sup>

As such, there is an increasing number of publications showing improved antibacterial efficacy employing GO-based antibiotic delivery systems. But the field remains fragmented, with conflicting results on cytotoxicity, size-dependent antibacterial mechanisms, stability under physiological conditions, GO-antibiotic synergy, and translational feasibility. Many existing reviews focus predominantly on antibacterial performance, often without critically comparing reported dose ranges, experimental models, and biological endpoints, which limits their relevance for pharmaceutical development. In addition, relatively few studies address *in vivo* behavior, long-term toxicity, clearance pathways, or regulatory considerations, despite their importance for clinical translation.

This review critically evaluates GO as an antibiotic nanocarrier by examining size, dose, and surface-chemistry-dependent antibacterial and cytotoxic effects, synthesizing mechanistic insights into GO-antibiotic synergy, identifying inconsistencies and unresolved controversies in the literature, and assessing realistic translational pathways and limitations.

## 2. Properties of GO

GO shown in Fig. 1 is an oxidative derivative of graphene and is typically produced in bulk from graphite through chemical

exfoliation. It has versatile applications due to its unique properties, such as chemical reactivity, dispersibility, high mechanical strength, intrinsic antimicrobial activity, and surface functionalization potential arising from its oxygen-containing functional groups (epoxy, carboxyl, and hydroxyl), which impart GO's hydrophilicity, chemical tunability, and biological properties.<sup>12</sup> GO has great potential in biomedical applications, including biomedicine and drug delivery. However, the suitability of GO in biomedical applications and antibiotic delivery is not intrinsic due to variability in GO's properties depending on its size, degree of oxidation, concentration, and environment.<sup>13</sup> Hence, the variable and inconsistent biological outcomes across studies, particularly in antibacterial efficacy and cytotoxicity assessments. GO demonstrates functionalization capability to bind different compounds due to its high surface area and functional groups, as evidence in its use in antibiotic carriers and targeted drug delivery systems.<sup>14</sup> In Table 1, a comparative review of the antibiotic-carrying capacity, intrinsic antibacterial activity, synergistic antibacterial activity, biocompatibility, and functionalization potential of GO and other nanomaterials, including reduced GO, carbon nanotubes, silver nanoparticles, polymeric nanoparticles, GO–Ag nanocomposite, metal oxide nanoparticles, and lipid-based nanoparticles, is shown. This comparison highlights the distinct advantages of GO, particularly high surface area, multifunctional antibacterial mechanisms, and surface tunability, alongside notable limitations related to toxicity, aggregation, and translational complexity, which must be considered when selecting an appropriate delivery platform. In Table 1 below, the star-based scoring system was assigned using defined semi-quantitative criteria. Antibiotic-carrying capacity was evaluated based on reported drug-loading efficiency and controlled-release performance. Intrinsic antibacterial activity was assessed using reported MIC/MBC values and/or bacterial reduction levels. Synergistic antibacterial activity was determined by assessing interactions with antibiotics, particularly the fractional inhibitory concentration index (FICI). Biocompatibility was evaluated based on *in vitro* cytotoxicity and hemolysis data. Functionalization potential was assessed based on the availability of reactive surface groups and demonstrated modification strategies.

### 2.1. Physicochemical properties of GO

GO's antibacterial properties depend heavily on its physicochemical characteristics, including lateral sheet size, alignment, surface charge, degree of oxidation, and dispersion stability.<sup>20,21</sup> Smaller GO nanosheets, despite possessing fewer oxygen groups, have greater oxidative potential and the capacity to surpass bacterial antioxidants such as  $\alpha$ -tocopherol. Larger GO nanosheets have superior wrapping capability; nevertheless, the antibacterial benefits can be negated by detaching GO from bacteria, as evidenced by experiments using *Escherichia coli*.<sup>22</sup> These findings indicate that antibacterial performance is not dictated by a single physicochemical parameter but by the interplay between size, surface chemistry, and exposure conditions. Dimensions and



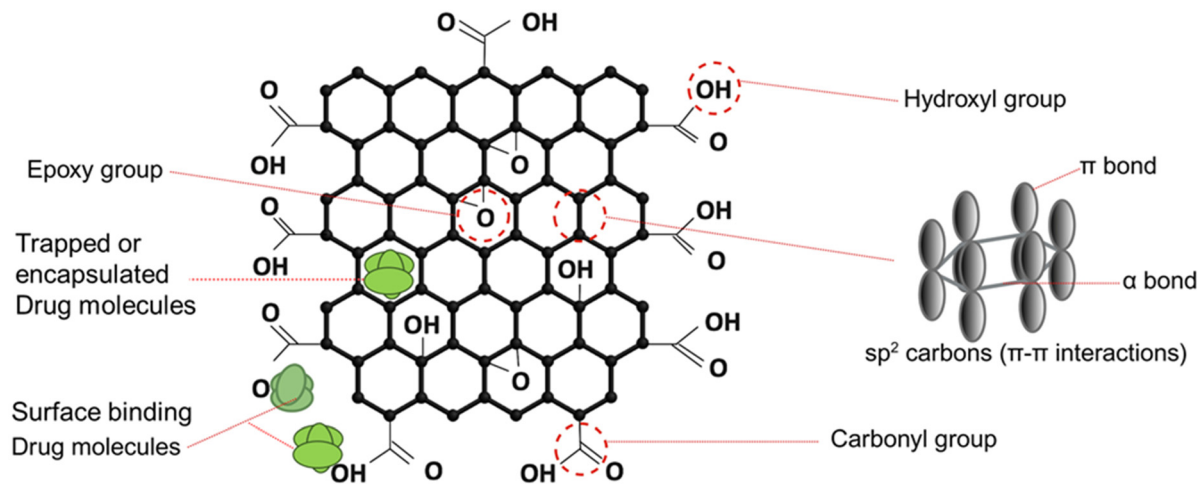


**Fig. 1** Structure of GO. GO contains  $sp^2$  and  $sp^3$  carbons ( $\pi$ - $\pi$  interactions with drug molecules) and oxygen functional groups (hydroxyl, carbonyl, and epoxy).

**Table 1** Comparison of nanomaterials for antibiotic delivery based on antibiotic-carrying capacity, intrinsic antibacterial activity, synergistic antibacterial activity, biocompatibility, and functionalization potential

Nanomaterial	Antibiotic carrying capacity	Intrinsic antibacterial action	Synergistic antibacterial activity	Biocompatibility	Functionalization potential	Ref
GO	★★★★★	★★★★☆	★★★★★	★★★★☆	★★★★★	15
GO-silver nanocomposite	★★★★★	★★★★★	★★★★★	★★★☆☆	★★★★★	16 and 17
Polymeric nanoparticles	★★★★★	★★☆☆☆	★★★☆☆	★★★★★	★★★★☆	18
Reduced GO	★★★★☆	★★★★☆	★★★★☆	★★★☆☆	★★★☆☆	19
Carbon nanotubes	★★★★☆	★★★☆☆	★★★☆☆	★★☆☆☆	★★★★☆	16
Silver nanoparticles	★★★☆☆	★★★★★	★★★★★	★★★☆☆	★★★☆☆	18
Lipid-based nanoparticles	★★★★★	★★★☆☆	★★★★☆	★★★★★	★★★★☆	8
Metal oxide nanoparticles	★★★☆☆	★★★☆☆	★★★☆☆	★★★☆☆	★★★☆☆	19

Each parameter was scored on a five-star (★★★★★) scale, where one star (★) indicates low or limited performance and five stars (★★★★★) indicate consistently high performance as reported in the literature.

morphology of GO affect its antibacterial efficiency, as rough GO surfaces facilitate effective contact with bacteria. Thus, optimization of the physicochemical properties of GO significantly influences its antibacterial efficacy through improved interactions with bacterial cells.<sup>14</sup> Importantly, such optimization must balance antibacterial potency with cytocompatibility, particularly for pharmaceutical applications.

The antibacterial activity of GO is primarily attributed to its sharp edges that disrupt bacterial membranes, the entrapment of cells, and the induction of oxidative stress,<sup>23</sup> all of which are influenced by the lateral size of the GO sheets. Smaller sheets have a higher edge density, which enhances their ability to cut bacterial membranes. In contrast, larger sheets with broader lateral dimensions are more capable of trapping microbial cells.<sup>24</sup> Interestingly, antibacterial due to oxidative stress appears unaffected by lateral dimensions, as addition of antioxidants such as ascorbic acid significantly reduced GO's antibacterial effects across all size groups,

suggesting that oxidative stress is a general and size-independent mechanism.<sup>25</sup>

Several studies provide different perspectives on how lateral sheet size impacts antibacterial activity. Liu *et al.* reported that larger GO sheets ( $>9 \mu\text{m}^2$ ) exhibited stronger antibacterial activity against *Escherichia coli* than smaller ones ( $0.010 \mu\text{m}^2$ ), especially at lower concentrations and shorter times.<sup>22</sup> Similarly, Vi *et al.* found that GO sheets larger than  $1 \mu\text{m}$  combined with Ag nanoparticles achieved higher bacterial killing than smaller GO-Ag sheets, largely due to enhanced entrapment of bacteria.<sup>26</sup>

In contrast, Perreault *et al.* observed that the antibacterial activity of smaller GO sheets (approximately  $0.01 \mu\text{m}^2$ ) was about four times more effective than that of larger ones (approximately  $0.65 \mu\text{m}^2$ ) in surface coatings, an effect attributed to increased oxidative damage caused by the smaller GO nanosheets.<sup>10</sup> Consistently, Ravikumar *et al.* emphasized that antibacterial efficacy is multifactorial, depending on purity,



sheet size, concentration, and exposure time, with smaller GO showing more oxidative stress due to higher defect density, and larger sheets wrapping and entrapment of bacterial cells.<sup>27</sup>

Overall, these results suggest that the size of the GO sheet critically regulates antibacterial mechanisms. Smaller nanosheets favor membrane disruption, larger sheets promote entrapment, and intermediate sizes achieve a balance of both effects. Thus, size-dependent mechanistic divergence represents a key design parameter for GO-based antibiotic delivery systems and underscores the need for standardized size reporting in antibacterial studies.

GO has good biological stability due to its hydrophilic and highly dispersible nature as a result of its oxygen-containing functional groups that promote stable aqueous suspensions and decrease aggregation.<sup>28</sup> Furthermore, the diverse surface chemistry of GO allows for functionalization, improving colloidal stability, biocompatibility, and stability in complicated biological settings such as physiological ionic strength and protein-rich media.<sup>29</sup> Additionally, GO's enormous specific surface area promotes effective drug adsorption and retention, while its inherent mechanical robustness helps maintain nanocarrier integrity during handling and biological interactions.<sup>29</sup> However, aggregation of GO under physiological salt concentrations and protein corona formation remain an important challenge under investigation for *in vivo* applications, as adsorbed biomolecules can significantly change GO's colloidal stability, cellular interactions, and biodistribution in biological contexts.<sup>30</sup>

## 2.2. Structural characteristics of graphene oxide and its interaction with antibiotics

The honeycomb-structured graphene monolayer made of single carbon atoms has drawn scientific interest because of its exceptional performance capabilities. The surface of GO contains epoxide, carboxylic acid, and hydroxyl functional groups within a single atomic layer.<sup>31</sup> This makes it water-soluble and gives scientists a large area to add antibiotics and modify groups for specific uses. These functional groups present in GO enable it to bind both water-insoluble and hydrophilic antibiotics, allowing targeted delivery of these drugs to specific target cells. Antibiotics containing aromatic or conjugated ring systems can interact with GO through  $\pi$ - $\pi$  stacking, and antibiotics bearing amine or hydroxyl groups form hydrogen bonds and electrostatic interactions with negatively charged carboxyl groups on GO. Additionally, covalent conjugation strategies can be employed *via* amide or ester linkages, further improving antibiotic stability and controlled release.<sup>32,33</sup> These interactions between GO and antibiotics help protect loaded antibiotics from enzymatic breakdown. Antibiotics adsorbed or immobilized on the GO surface protect vulnerable functional groups from enzymatic degradation by  $\beta$ -lactamases. The adsorption of antibiotics *via*  $\pi$ - $\pi$  stacking, hydrogen bonding, covalent bonding, and electrostatic interactions can create steric hindrance and reduce antibiotic molecular mobility, thereby limiting enzyme accessibil-

ity and slowing enzymatic hydrolysis.<sup>34</sup> Furthermore, GO-based nanocarriers allow for the localized and regulated release of antibiotics at the site of bacterial infection, reducing the drug's premature exposure to degrading enzymes found in the biological milieu.<sup>35</sup> This improves antibiotic stability and local concentrations near bacterial cells, resulting in increased antibacterial activity against resistant infections. Thus, modification and antibiotic loading on GO achieved through the use of covalent and electrostatic bonds, hydrogen bonds, van der Waals forces, and  $\pi$ - $\pi$  stacking is highly beneficial in next-generation antibiotic development.<sup>36,37</sup> For example, controlled-release properties that are appropriate for colon-specific drug delivery have been demonstrated using GO-based hydrogels to encapsulate vancomycin. GO-based systems for controlled antibiotic release, customized to release antibiotics at specific locations within the body, improve therapeutic outcomes due to their pH-responsive characteristic.<sup>38</sup> Nevertheless, many of these systems remain proof-of-concept and lack systematic pharmacokinetic and biodistribution evaluation. In GO-based functionalized systems, the carboxyl functional group, which is abundant and highly reactive, is frequently used for surface functionalization of GO, mostly through dehydration involving the removal of a hydroxyl and an amino group to form an amide bond.<sup>15,39</sup>

## 2.3. Biocompatibility, low toxicity, and target delivery

GO does not show universal biocompatibility, but rather dose, size, and cellular model-dependent cytocompatibility according to several *in vitro* investigations. For instance, Chang *et al.* showed that GO concentrations below 20  $\mu\text{g mL}^{-1}$  did not cause significant oxidative stress or membrane damage to human lung epithelial (A549) cells; however, higher dosages produced detectable cytotoxic reactions in A549 cells.<sup>38</sup>

Also, Russier *et al.* demonstrated that human macrophages have a far higher tolerance to GO than their murine macrophages, with lower ROS production and immunological activation. They also found that bigger GO flakes mostly interacted with the cell membrane, while smaller GO sheets ( $\leq 300$  nm) were more effectively absorbed and caused higher oxidative stress and cytokine release.<sup>39</sup>

Similar differences were seen in GO sensitivity between immortalized ARPE19 cells, primary human RPE cells, and retinal pigment epithelial cells generated from embryonic stem cells (ESC-RPE). While ESC-RPE and primary hRPE cells only showed notable viability loss at GO levels  $\geq 100$   $\mu\text{g mL}^{-1}$ , ARPE19 cells showed reduced viability at concentrations as low as 50  $\mu\text{g mL}^{-1}$ . These results imply that while stem-cell-derived and primary human cells offer a more physiologically appropriate evaluation of safety, immortalized cell lines may overestimate GO cytotoxicity.<sup>40</sup> Collectively, these studies confirm that variations in reported GO cytotoxicity result from a combination of dose, physicochemical characteristics, and the selection of the cellular model. This emphasizes the need for consistent toxicity standards and human-relevant models for assessing GO for pharmaceutical applications.<sup>42</sup>



Fortunately, surface modifications have consistently reduced the toxicity effects of GO.<sup>43</sup> Functionalizing GO with biocompatible coatings, including dextran,<sup>44</sup> gallic acid,<sup>45</sup> bovine serum albumin,<sup>46</sup> polyethylene glycol,<sup>47</sup> and other biocompatible polymers, improved colloidal stability and hydrophilicity, as well as less nonspecific interactions between GO and cellular membranes.<sup>44</sup> In a study to assess the cytotoxicity of GO flakes and GO-amoxicillin conjugates, the cell line of mice fibrosarcoma WEHI 164 cultivated without GO served as the control and had 94.1% viable cells. In comparison, mice fibrosarcoma WEHI 164 cells exposed to GO flakes or GO linked to amoxicillin showed only modestly lower viability (>90% viable cells), showing that neither formulation had a major cytotoxic effect.<sup>51</sup> However, GO-antibiotics conjugates offer the advantage of target delivery, facilitating localized antibiotic accumulation and decreasing antibiotic off-target effects.<sup>52</sup> However, *in vivo* targeting efficiency, off-target accumulation, and long-term safety remain insufficiently explored (Fig. 2).

#### 2.4. Antimicrobial activity

GO exhibits antibacterial activity against a wide range of bacteria; nevertheless, reported results vary widely depending on assay type, concentration, exposure time, and dispersion stability. Reported growth inhibition experiments, such as inhibition zone measurement and optical density-based growth suppression, primarily demonstrate bacteriostatic effects rather than bactericidal effects. Unfortunately, these distinctions are not usually well described.<sup>47</sup> GO has been reported to

exhibit strong bacteriostatic action at low to moderate concentrations across various exposure times, inhibiting bacterial growth without causing immediate cell death. For instance, growth inhibition of *Staphylococcus aureus* has been observed between 2 and 24 hours of GO exposure, whereas *Pseudomonas aeruginosa* showed substantial growth suppression as early as 2 h after treatment.<sup>48</sup> Researchers revealed that the bacteriostatic effect is substantially concentration dependent, with *Staphylococcus aureus* consistently more sensitive than *Escherichia coli*, resulting in progressively bigger inhibition zones as GO concentration increased.<sup>49–52</sup> Similar inhibitory action has been shown for oral pathogens: *Enterococcus faecalis* and *Streptococcus mutans*, which are involved in both localized and systemic infections.<sup>49–52</sup> He *et al.* found that GO nanosheets at 20–40  $\mu\text{g mL}^{-1}$  reduced the proliferation of *Porphyromonas gingivalis* and *Fusobacterium nucleatum*, while *Streptococcus mutans* required higher doses (80  $\mu\text{g mL}^{-1}$ ) for substantial suppression.<sup>45,53</sup> To visually support this dose-dependent inhibition and cell damage in oral pathogens, Fig. 3 compiles activity/viability outcomes with fluorescence- and TEM-based evidence of membrane compromise.

These bacteriostatic effects were linked to reversible processes such as oxidative stress generation, interference with membrane integrity, and reduced nutrition transfer, limiting bacterial multiplication without causing immediate cell death. At higher concentrations and longer exposure times, GO switches from growth inhibition to bactericidal activity, resulting in irreversible cellular damage and bacterial death. In time-kill studies of GO against methicillin-resistant

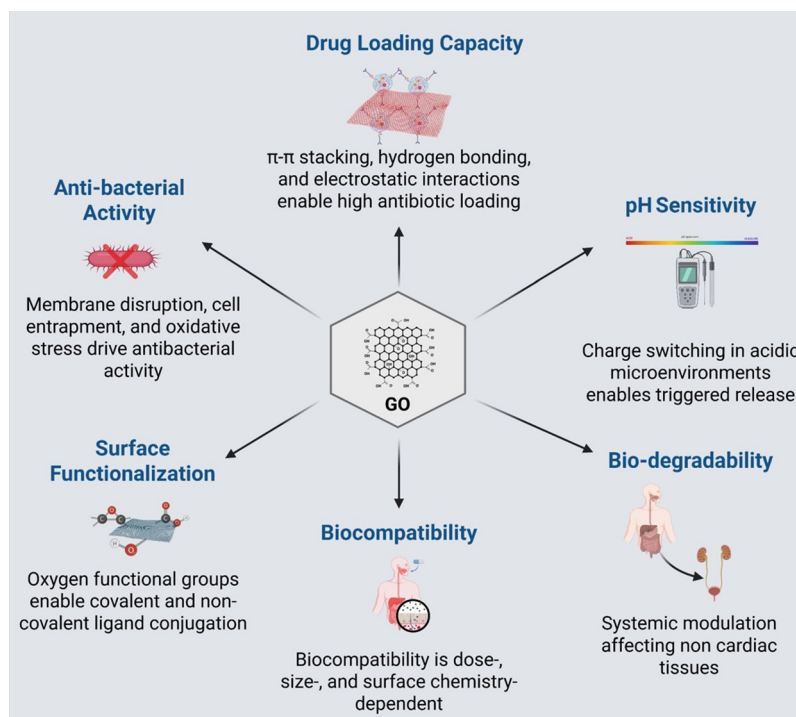
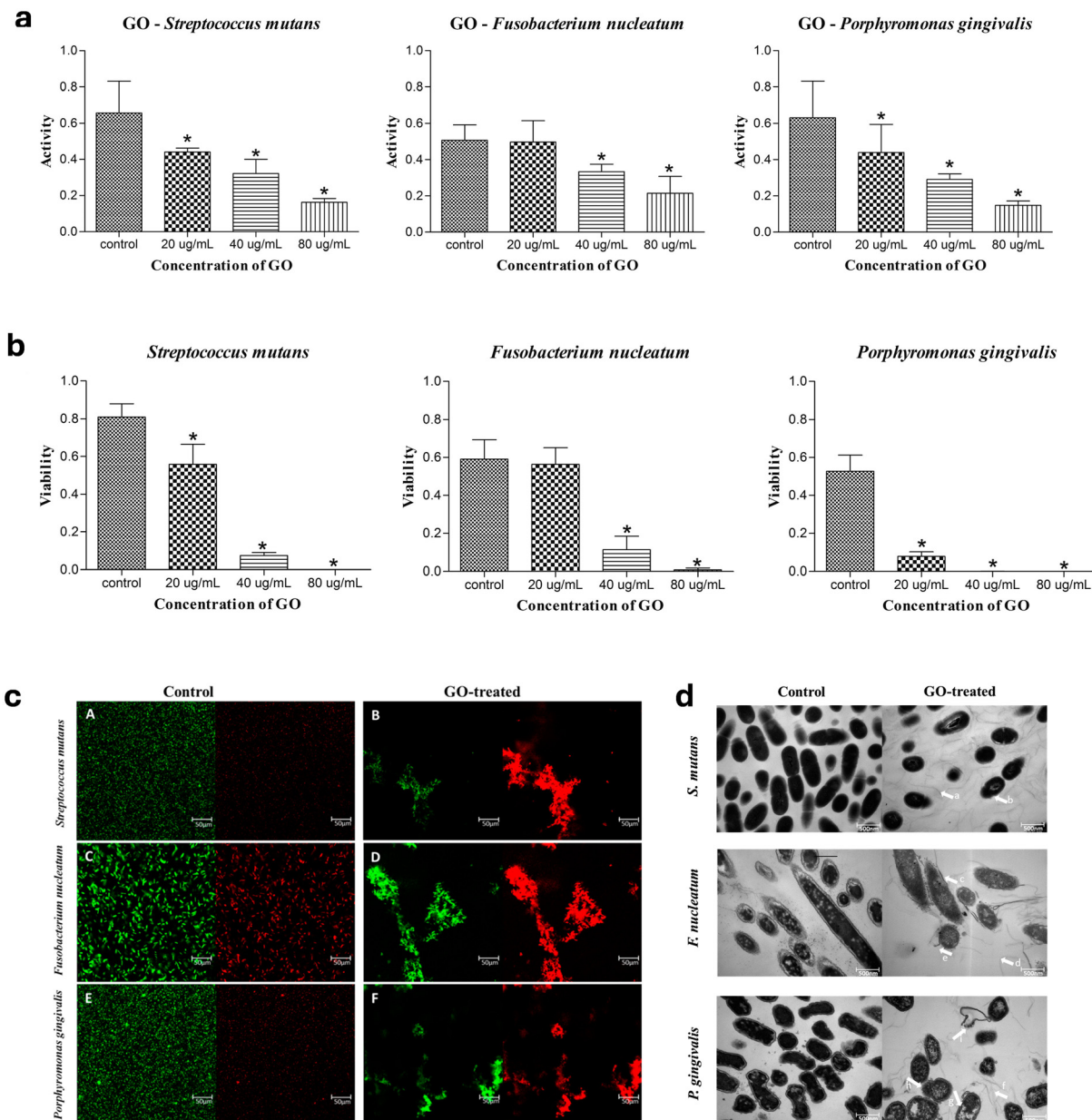


Fig. 2 Graphene oxide (GO) exhibits unique physicochemical properties that make it highly suitable for biomedical applications.





**Fig. 3** Dose-dependent antibacterial activity of graphene oxide against dental pathogens with live or dead and ultrastructural evidence of membrane damage. (a)–(d) GO activity against dental pathogens after 2 h exposure (20–80  $\mu\text{g mL}^{-1}$ ): (a) MTT-based antibacterial activity for *S. mutans*, *F. nucleatum*, and *P. gingivalis*; (b) CFU-based viability quantification; (c) live or dead fluorescence imaging (SYTO 9/PI; scale bar = 50  $\mu\text{m}$ ); and (d) TEM images comparing control vs. GO-treated cells (scale bar = 500 nm). Adapted from ref. 53, Copyright 2015 American Chemical Society.

*Staphylococcus aureus* strains, prolonged exposure or higher concentrations resulted in irreversible membrane damage, cellular leakage, and eventual bacterial cell death.<sup>60</sup> Also, rapid killing has been recorded, with *Mycobacterium smegmatis*, *Escherichia coli*, and *Staphylococcus aureus* reduced by 99% within 15 minutes of GO exposure, indicating a fast-acting bactericidal action.<sup>54</sup> However, it is worth mentioning that the early killing of bacteria involved a higher dose of GO. Furthermore, GO has been shown to kill *Escherichia coli*, *Streptococcus mutans*, *Staphylococcus aureus*, and *Enterococcus faecalis* at concentrations of 300–500  $\mu\text{g mL}^{-1}$  and incubation

durations of up to 60 minutes.<sup>55</sup> Among these, *Escherichia coli* was the most susceptible, with mortality rates of up to 96%, and *Staphylococcus aureus* was the most resistant, with mortality rates of around 55% under the same conditions. These dose-dependent transitions from bacteriostatic to bactericidal behavior are critical for interpreting experimental outcomes and comparing studies.

Compared with traditional antibiotics, GO exhibited broad-spectrum antibacterial activity, including against antibiotic-resistant bacteria.<sup>1</sup> GO reduced the growth of *Escherichia coli*, *Klebsiella pneumoniae*, *Pseudomonas aeruginosa*, *Proteus mir-*



*abilis*, *Serratia marcescens*, and *Staphylococcus aureus*, all of which were resistant to amoxicillin, cotrimoxazole, cefixime, and imipenem.<sup>1</sup> While typical antibiotics like ciprofloxacin, ceftriaxone, azithromycin, and gentamycin showed inhibition zones ranging from 7–29 mm, GO exhibited far greater zones of inhibition (27–41 mm) against the same bacteria.<sup>1</sup> The experimental evidence supporting GO's intrinsic antibacterial and antibiofilm activity across MDR isolates and chronic-wound microorganisms is summarized in Fig. 4.

However, variations in the reported bacteriostatic and bactericidal activity of GO are associated with variations in GO concentration, exposure time, and bacterial strain.<sup>56</sup> And the high concentrations required for antibacterial activity in some of these studies raise concerns regarding translational feasibility. Table 2 provides a summary of research testing the antibacterial activity of GO.

GO-mediated antibacterial mechanisms include bacterial cell membrane disruption, entrapment of bacterial cells, oxidative stress induction, and charge-transfer-induced lipid extraction.<sup>59,60</sup> This is evident in numerous studies emphasizing the potent antibacterial properties of GO, but the efficacy of GO is contingent upon the type of bacteria and cannot be generalized to all bacteria.<sup>22,61</sup> Studies indicate heightened susceptibility of Gram-positive bacteria to the entrapping effect by GO owing to their structural characteristics, which include teichoic acids and amino acids inside the peptidoglycan layer. Conversely, Gram-negative bacteria, like *Escherichia coli*, may necessitate elevated concentrations of GO for efficient trapping owing to their protective outer layer.<sup>62–65</sup> Oxidative stress as a mechanism of antibacterial action by GO arises *via* reactive oxygen species (ROS) generation and antioxidant depletion, facilitated by electron transfer between bacterial membranes and GO's oxygenated basal planes.<sup>66–69</sup> The electron transfer method, particularly with immobilized GO on surfaces, effectively induces oxidative stress without the need for GO to infiltrate or encapsulate bacteria. The basal plane of GO is crucial for antibacterial activity, facilitating effective contact with bacterial cells and resulting in charge transfer and ROS generation. GO demonstrates variable antibacterial effectiveness against Gram-positive and Gram-negative bacteria. Findings from various studies suggest that Gram-negative bacteria are more sensitive to oxidative stress due to their thinner peptidoglycan layer, while Gram-positive bacteria's susceptibility arises due to the lack of an outer membrane.<sup>26,54,70</sup> These mechanistic differences highlight the importance of tailoring GO design to specific bacterial targets rather than assuming broad-spectrum equivalence (Fig. 5).

### 3. Mechanisms of antibiotic loading and release

GO possesses a hydrophilic surface, abundant oxygen-containing functional groups, high surface area, and flexible surface chemistry, which collectively make its usage in drug delivery platforms feasible. In antibiotic delivery, GO interacts with

antibiotics through multiple reversible and irreversible interactions, such as hydrogen bonds, covalent bonds,  $\pi$ - $\pi$  stacking interactions, and electrostatic interactions. This makes GO suitable for tunable antibiotic loading and target delivery rather than just a passive antibiotic transport platform.<sup>35</sup> Interestingly, these interactions are not universally beneficial, as excessively strong binding can suppress antibiotic bioavailability and reduce antibacterial efficacy, particularly in systems relying on passive release.<sup>71</sup> Thus, the strength and reversibility of these interactions have a direct influence on the release kinetics, antibacterial efficacy, and potential synergistic or antagonistic outcomes in GO-antibiotic systems, thereby necessitating careful and mechanism-informed design of GO-antibiotic delivery systems.

#### 3.1. Adsorption mechanism and drug loading

Non-covalent functionalization is widely used because it preserves the intrinsic physicochemical properties and basal plane structure of GO, thereby maintaining GO's mechanical integrity and antibacterial activity. It consists mainly of hydrogen bonds, electrostatic interactions, and  $\pi$ - $\pi$  interactions.<sup>12</sup> Non-covalent functionalization achieves the main goal of preserving GO properties throughout the antibiotic delivery processes. According to research investigations, non-covalent coupling improves drug loading abilities, regulates sustained drug delivery, and enhances biological compatibility. This technique is particularly useful for antibiotic delivery because it enables drug release to be initiated by environmental changes such as pH, ionic strength, or competitive interaction with biomolecules.<sup>72–74</sup> This responsiveness is especially relevant in infected tissues, where acidic microenvironments and high protein content can trigger drug desorption. For instance, cephalexin has been immobilized on GO surfaces *via* non-covalent adsorption and showed enhanced inhibition of both *Escherichia coli* and *Staphylococcus aureus*.<sup>75</sup> The functionalization of GO through non-covalent interactions can be achieved by permitting its negatively charged surface to bind with positively charged nanomaterials and functional entities such as liposomes, chitosan, and metal nanoparticles before adsorption of antibiotics onto the nanocomposite.<sup>12,44,76</sup>

#### 3.2. Covalent bonding and drug loading

A better way to modify GO through functionalization involves surface functional groups that can undergo covalent modifications. Covalent functionalization of GO occurs through its surface hydroxyl, carboxylic, and epoxide groups by utilizing processes such as esterification,<sup>15</sup> amidation,<sup>77</sup> acetylation, isocyanation, diazotization, and other methods.<sup>78</sup> Covalent bonding techniques allow for a stronger and more stable attachment of medicines to GO than non-covalent ways. This approach allows for more precise control over the antibiotic release from the GO. Chemically attaching pharmaceuticals to the surface of GO allows the drug delivery mechanism to be adjusted to specific therapeutic needs. The covalent attachment ensures that the drug remains bound to the carrier until it reaches its target location, thereby reducing premature



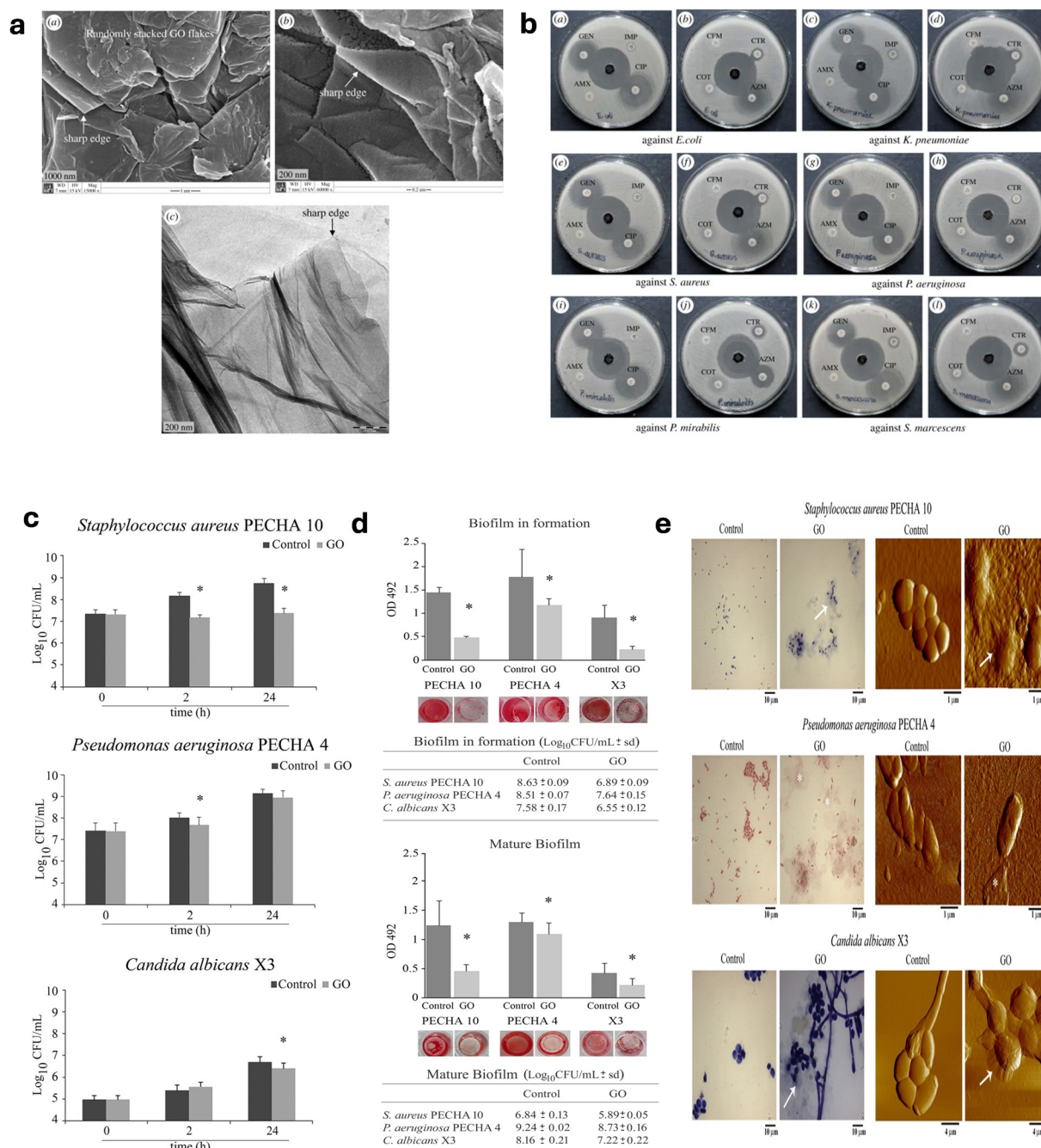


**Fig. 4** Representative evidence for GO antibacterial and antibiofilm activity: nanosheet morphology, broad-spectrum inhibition of MDR isolates, and suppression of planktonic and biofilm growth with microscopy-supported interactions. (a) FESEM/TEM characterization of GO showing stacked GO flakes, exposed sharp edges, and thin GO nanosheets. (b) Disc diffusion-based *in vitro* antibacterial activity comparing GO with commercial antibiotics against multidrug-resistant clinical isolates: *E. coli* (a and b), *K. pneumoniae* (c and d), *S. aureus* (e and f), *P. aeruginosa* (g and h), *P. mirabilis* (i and j), and *S. marcescens* (k and l). Adapted from ref. 1, Copyright 2020 The Royal Society. (c)–(e) Antimicrobial and antibiofilm efficacy of GO ( $50 \text{ mg L}^{-1}$ ) against chronic wound microorganisms: (c) time-dependent inhibition of planktonic growth ( $\log_{10} \text{ CFU mL}^{-1}$ ) for *S. aureus* PECHA 10, *P. aeruginosa* PECHA 4, and *Candida albicans* X3; (d) inhibition of biofilm in formation (A) and mature biofilm (B) quantified by biomass or representative images and CFU enumeration; and (e) representative Gram staining and AFM images indicating GO wrapping and GO-associated surface coverage. Adapted from ref. 48, Copyright 2018 American Society for Microbiology.

release.<sup>79</sup> Covalent modification serves the essential purpose of improving GO's drug delivery system (DDS) surface characteristics together with their biocompatibility, loading

efficiency, and release behavior for biomedical implications.<sup>44</sup> Carboxyl functional groups, found in great abundance, serve as the most commonly employed covalent modification points



**Table 2** Bacterial growth suppression using GO

Bacteria tested	Dose ( $\mu\text{g mL}^{-1}$ )	Effectiveness/ observations	Ref.
<i>Escherichia coli</i> , <i>Klebsiella pneumoniae</i> , <i>Pseudomonas aeruginosa</i> , <i>Proteus mirabilis</i> , <i>Serratia marcescens</i> , and <i>Staphylococcus aureus</i>	1000 $\mu\text{g mL}^{-1}$	Ciprofloxacin, ceftriaxone, azithromycin, and gentamycin produced between 7–29 mm zones of inhibition against the bacteria, while GO produced zones of inhibition between 27–41 mm against the bacteria tested	1
<i>Staphylococcus aureus</i> , <i>Pseudomonas aeruginosa</i>	Not specified	The growth suppression was significant in <i>Staphylococcus aureus</i> at 2 and 24 hours, while <i>P. aeruginosa</i> at 2 hours.	48
<i>Mycobacterium smegmatis</i> , ( <i>Escherichia coli</i> ), <i>Staphylococcus aureus</i>	Not specified	99% reduction in bacterial viability within 15 minutes.	57
<i>Staphylococcus aureus</i> , <i>Escherichia coli</i> , <i>Pseudomonas aeruginosa</i>	250–1500 $\mu\text{g mL}^{-1}$	Concentration-dependent inhibition: higher concentrations gave higher zones of inhibition	58
<i>Streptococcus mutans</i> , <i>Porphyromonas gingivalis</i> , <i>Fusobacterium nucleatum</i> ( <i>F. nucleatum</i> )	20, 40, 80 $\mu\text{g mL}^{-1}$	Complete inhibition of <i>P. gingivalis</i> and <i>F. nucleatum</i> at 40 $\mu\text{g mL}^{-1}$ ; <i>S. mutans</i> was suppressed at 80 $\mu\text{g mL}^{-1}$ .	53
<i>Enterococcus faecalis</i> ( <i>E. faecalis</i> ), <i>Staphylococcus aureus</i> , <i>Escherichia coli</i> , <i>S. mutans</i>	300, 500 $\mu\text{g mL}^{-1}$	<i>Escherichia coli</i> : 96% mortality at 500 $\mu\text{g mL}^{-1}$ for 60 min; <i>Staphylococcus aureus</i> : 55% mortality; extended times showed diminishing effects except for <i>E. faecalis</i> .	52

for GO surfaces. Reagent initiation occurs first in carboxyl functionalization before the dehydration process forms bonds as either esters or amide groups. The activation process uses four main reagents, which are hexafluorophosphate and thionyl chloride ( $\text{SOCl}_2$ ), and 1-ethyl-3 (3-dimethylaminopropyl)-carbodiimide (EDC) together with *N,N*-dicyclohexylcarbodiimide (DCC). In a GO-Amoxicillin complex, GO is linked to Amoxicillin (AMOX) through a Gly-Gly-Leu peptide linker. GO's hydroxyl groups were activated using divinyl sulfone to create the complex, and *N,N'*-Dicyclohexylcarbodiimide was used to activate the linker's carboxyl groups. This process facilitates a stable covalent attachment of AMOX to GO. Upon attachment, the GO-AMOX complex was contained within a hydrogel matrix with bromelain (BROM), an enzyme that cleaves the peptide linker and regulates AMOX release. The AMOX release speed depended on BROM content within the hydrogel, thus enabling con-

trolled release of AMOX. An optimal enzyme environment enables the system to release more than 90% of AMOX during 24 hours. The controlled release method specifically reaches affected areas particularly well for dental uses, which yield complex bacterial structures. The device achieves improved infection treatment results through its long-term antibacterial action at infection sites, reducing the required doses during the treatment of periodontal and endodontic diseases (Fig. 6).<sup>80–82</sup>

### 3.3. Stimulus-responsive release systems

Stimulus-responsive drug delivery has emerged to enhance both drug delivery precision and minimize systemic side effects. They exploit internal stimuli (pH, enzymes, redox reactions) and external triggers (temperature, magnetic fields) to trigger antibiotic release.<sup>83</sup> GO is ideal for stimulus-responsive administration because its surface chemistry may be easily altered to adapt to environmental stimuli.<sup>35</sup> pH-responsive release is particularly important for antibiotic administration since infection sites frequently exhibit localized acidity as a result of bacterial metabolism and inflammation.<sup>84</sup> Enzyme-responsive systems allow for more selective drug release in settings rich in bacterial or host-derived proteases.<sup>85</sup> Stimulus-responsive GO systems enable regulated and spatially focused release, increasing therapeutic efficacy while reducing off-target toxicity.<sup>84</sup> Nonetheless, the majority of published systems rely on single-stimulus activation, while multi-stimulus-responsive GO-antibiotic systems are understudied, despite their potential to improve specificity and therapeutic control.

### 3.4. Kinetics of antibiotic release

The rate of antibiotic release from GO-based nanocarriers depends on functionalization type, drug-carrier binding force, and the surrounding physiological conditions. Drug release kinetics typically follow a regulated release profile, which can be altered by adjusting GO functionalization.<sup>86</sup> In adsorption-based drug release, the nature of the interactions between the drug and the functional groups on the GO surface frequently governs the release rate.<sup>86</sup> Covalent bonding strategies often result in slower drug release than non-covalent approaches because the drug is more strongly linked to the carrier. Stimuli-responsive devices can further regulate the release profile by delivering the drug to the target region in a regulated manner dependent on the triggering stimulus.<sup>86</sup> The release kinetics of antibiotics from GO-based systems are typically governed by a combination of diffusion, desorption, and pH-responsive behaviors, allowing for both rapid initial release and prolonged therapeutic action. Antibiotic release from GO commonly follows non-Fickian (anomalous) kinetics, influenced by diffusion and matrix relaxation. These behaviors are modeled using the Peppas-Sahlin model, Ritger-Peppas model, Hopfenberg model, Narasimhan-Peppas model, zero-order, and first-order kinetics models.<sup>6</sup>

In a study involving the release of AMOX from NaAlg-GO/CS@AMX, the release kinetics of AMOX best fit the Korsmeyer-Peppas model, confirming Fickian diffusion-con-





**Fig. 5** Mechanism of antibacterial action of GO. GO kills bacterial cells via cell entrapment, ROS-induced oxidative stress, membrane disruption leading to cell lysis, and physical penetration through the bacterial cell wall.

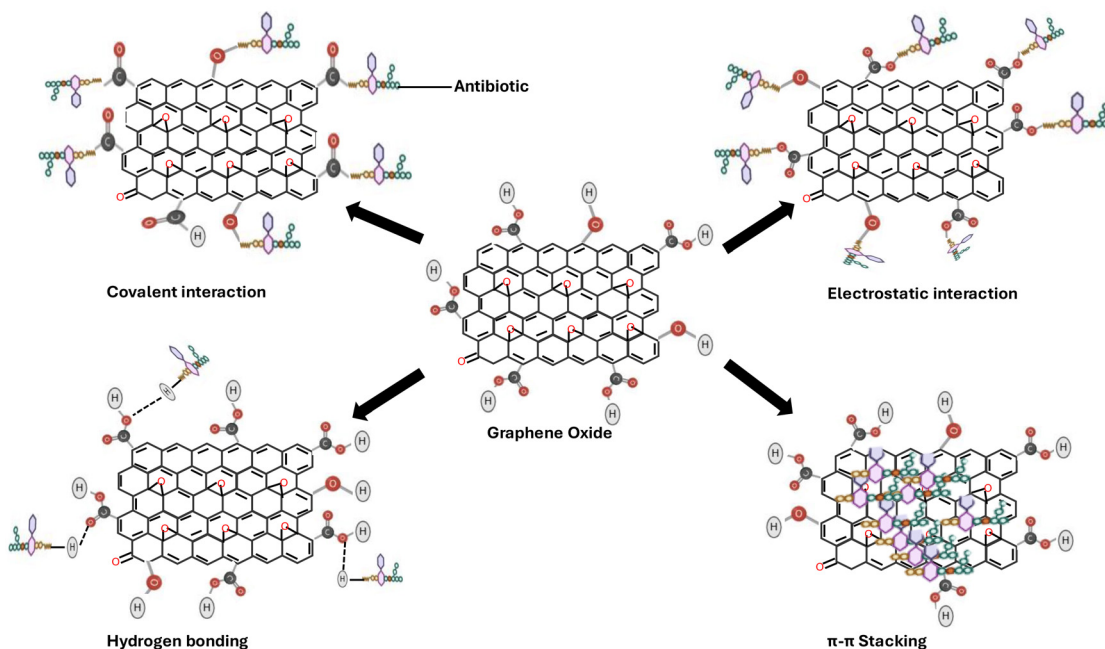


**Fig. 6** Schematic representation of the mechanisms of antibiotics loading on GO. Covalent interactions, electrostatic interactions, hydrogen bonding, and  $\pi$ - $\pi$  stacking facilitate antibiotic attachment and stabilization on the surface of GO.

trolled release.<sup>87</sup> Furthermore, Trusek *et al.* reported a multi-phase release behavior for GO-linked antibiotics containing enzymatically cleavable peptide linkers, with an initial burst phase followed by sustained and extended release. Such multi-phase release profiles are especially useful in antibiotic

therapy, where a large initial dose decreases bacterial load, followed by prolonged exposure to inhibit regrowth and biofilm development.<sup>45,88</sup> Similarly, a multifunctional nanocomposite system consisting of GO, chitosan, and silver nanoparticles provided a pH-controlled drug release. The system, capable of



controlled release of both a single drug and a dual drug, featured a burst drug release for 10 h and a more stabilized release (70–80%) after 40–50 h.<sup>89</sup> These findings highlight the potential of GO-based platforms for programmable antibiotic delivery to prolonged antibacterial action and biofilm disruption.

## 4. Application of GO in antibiotic delivery

A detailed summary of GO's biomedical applications is illustrated in Fig. 7. Targeted drug delivery utilizes GO's tunable surface chemistry to deliver therapeutic agents specifically to diseased tissues, enhancing therapeutic efficiency while reducing systemic side effects.<sup>32</sup> This targeting capability is pertinent in antibiotic delivery, where localized infections and biofilm-associated illnesses require elevated local antibiotic concentrations. Mohammadi Tabar *et al.* formulated a polyethylene glycol-functionalized GO (GO-PEG) nanocarrier and used it to deliver penicillin and oxacillin, two  $\beta$ -lactam antibiotics that are ineffective against methicillin-resistant *Staphylococcus aureus* (MRSA). The study revealed significant drug loading of 81% for penicillin and 92% for oxacillin, attributed to the antibiotics'  $\pi$ - $\pi$  stacking and hydrogen bonding interactions with the GO surface. Importantly, the GO-PEG-antibiotic systems demonstrated sustained drug

release for roughly 6 days, as opposed to the fast release reported with the free antibiotics. Additionally, the antibacterial testing revealed much greater suppression of MRSA (about 80–85%), compared to either free antibiotics or GO-PEG alone.<sup>90</sup> Several other recent investigations have shown that GO and its functionalized derivatives can be used as excellent antibiotic delivery platforms, with high drug loading, controlled release, and increased antibacterial activity against resistant bacteria.<sup>9,91,92</sup> GO has equally been explored as a carrier in gene delivery and gene therapy, chemotherapy,<sup>93</sup> and regenerative medicine,<sup>94</sup> due to its ability to complex nucleic acids and facilitate cellular internalization, improve drug solubility and controlled release, and reduce off-target cytotoxicity.<sup>93</sup> GO can also enhance cell adhesion, proliferation, and differentiation owing to its biocompatibility and mechanical stability.<sup>94</sup> Although these applications are outside the direct scope of antibacterial therapy, they provide foundational insight into GO-biomolecule interactions that inform antibiotic loading strategies. GO's multifaceted role in advancing both therapeutic and diagnostic technologies in medicine is highlighted in Fig. 7.<sup>95,96</sup>

### 4.1. GO-antibiotic combination therapy for multidrug-resistant bacteria

GO is an intriguing candidate for combination therapies for patients with multidrug resistance (MDR) due to its unique physicochemical properties and intrinsic antibacterial activity.

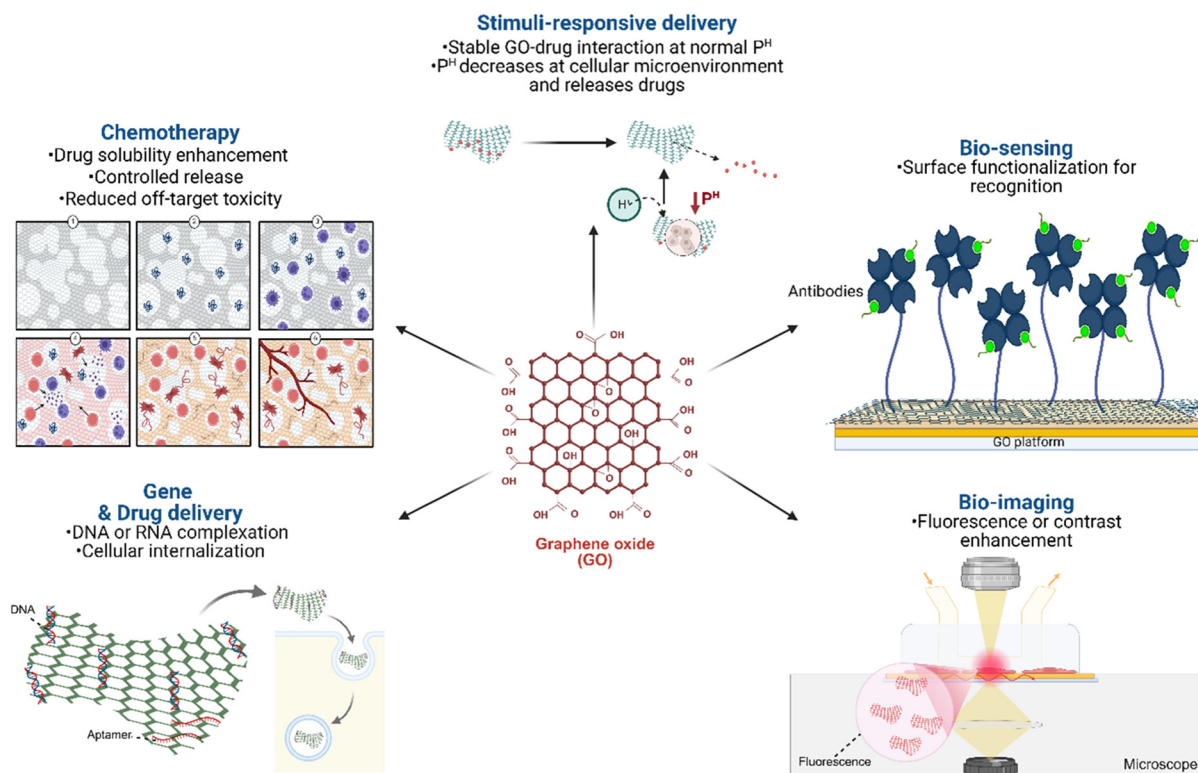


Fig. 7 Overview of biomedical applications of GO, including targeted drug delivery, stimuli-responsive drug delivery, chemotherapy, regenerative medicine, bioimaging, biosensing, gene delivery, and gene therapy.



Unlike inert carriers, GO can actively contribute to bacterial growth suppression and killing while simultaneously enhancing antibiotic stability, delivery, and overall efficacy. Thus, medical professionals may use GO as an essential treatment component that functions in combination therapies for MDR bacterial treatments. The distinctive applications of GO in combination therapy against MDR are discussed in the following sections.<sup>41</sup>

GO increases the antibacterial action of traditional antibiotics through three distinct mechanisms. First of all, it can entrap bacterial cells, isolating them and causing death due to starvation from nutrients.<sup>25</sup> Through direct contact, GO also induces bacterial cell death by disrupting bacterial cell membranes with its sharp edges.<sup>18</sup> Lastly, the functional groups on GO can cause bacterial cell death through oxidative stress.<sup>26</sup> When combined with antibiotics, these mechanisms increase bacterial membrane permeability, facilitate intracellular antibiotic penetration, and elevate local drug concentration at the bacterial surface. GO delivers antibiotics into bacterial cells by disrupting cell membrane integrity and the cell wall. This allows antibiotics to interact with bacteria's ribosomes, mitochondria, proteins, DNA, and enzymes. It can also entrap bacterial cells, allowing antibiotics to act on bacterial cells better due to increased local antibiotic concentration. For instance, meropenem-loaded GO (Mrp-GO) exhibited enhanced antibacterial activity against carbapenem-resistant Gram-negative bacteria with minimal cytotoxicity to human cells in comparison to meropenem alone.<sup>97</sup> The enhanced antibacterial activity can be attributed to GO-induced

membrane destabilization, which overcomes reduced antibiotic uptake associated with carbapenem resistance (Fig. 8).

Researchers Trusek and Kijak investigated the use of GO as a vehicle for antibiotic delivery. They used a Gly-Gly-Leu peptide linker to attach the semi-synthetic  $\beta$ -lactam antibiotic AMOX to GO covalently, and incorporated it into a hydrogel with Bromelain, an enzyme that degrades the covalent bond at 37 °C and pH 6.6. The resulting hydrogel effectively inhibited the growth of the *Enterococcus faecalis* strain, a pathogen responsible for periodontal and root canal diseases. According to the results, the amount of the Bromelain enzyme determined the rate of AMOX release. The study highlights that enzyme-responsive GO systems are effective platforms for site-specific antibiotic release in periodontal and endodontic infections.<sup>45</sup> Similarly, the antibacterial efficacy of GO combined with DAP (ciprofloxacin and metronidazole) demonstrated superior antibacterial efficacy against *Enterococcus faecalis* than either GO or DAP alone. The DAP treatment reduced bacterial levels by 98.22% during the first day before eliminating all bacteria within 14 days. GO demonstrated a 42.78% reduction in bacterial count from the original level during the first day, which increased to 82.90% after seven days and achieved 97.54% elimination after two weeks. The combined antibacterial effect of GO-DAP eliminated *E. faecalis* bacteria within 24 hours, thus demonstrating its potential application in treating root canal infections.<sup>32</sup> This study revealed the role of GO in accelerating antibiotic efficacy and not merely as a carrier that prolongs antibiotic exposure.

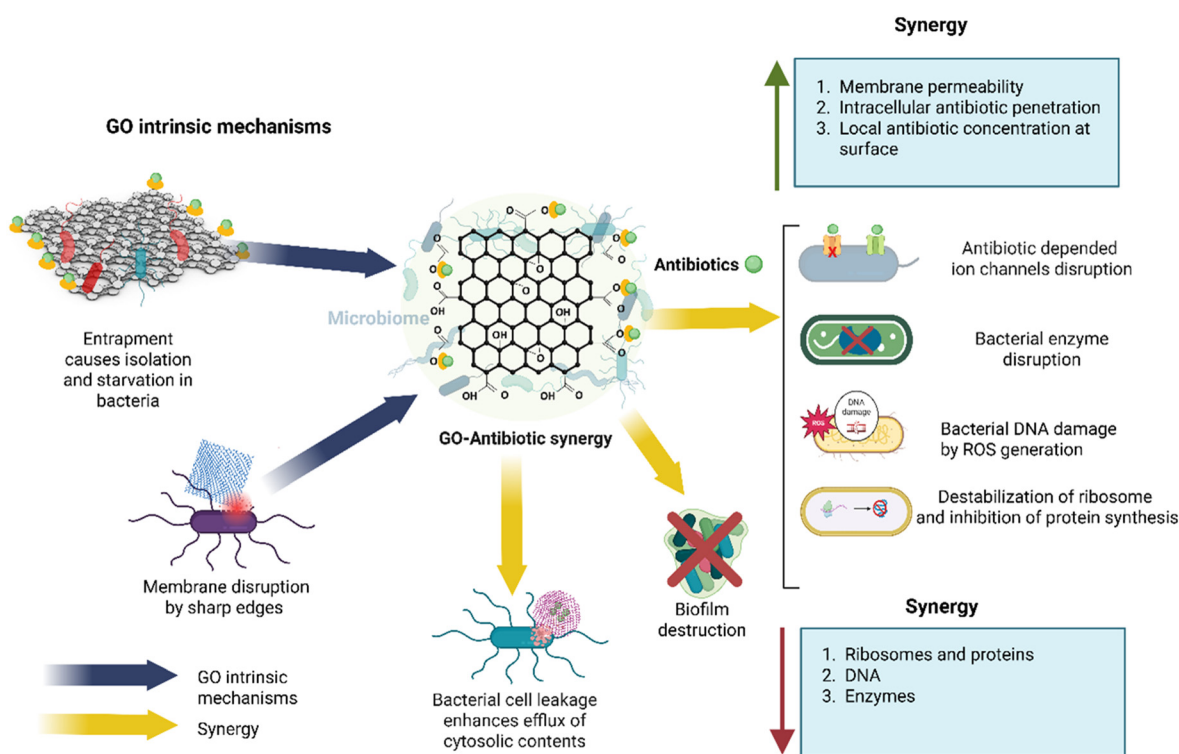


**Fig. 8** The illustration of the synergistic antibacterial action of GO-loaded antibiotics through antibiotic-dependent bacterial cell leakage, loss of membrane integrity, bacterial entrapment, and ion channel disruption.



Sengupta *et al.* conducted original research that introduced a groundbreaking pH-sensitive drug release system by combining GO with alginate. Alginate-GO-Ciprofloxacin (CIP) was used to evaluate CIP release for gastrointestinal infection treatment in various pH solutions, ranging from pH 7 (neutral) to pH 2.8 (acidic) and back to pH 7.4 (physiological conditions).<sup>6</sup> GO incorporation into the system created more CIP absorption areas as well as smaller pores that function better at different pH values, and increased CIP encapsulation efficiency by 16% higher. Notably, strong hydrogen bonding under acidic conditions restricted premature drug release, while alkaline conditions promoted matrix swelling and controlled drug liberation.<sup>6</sup>

Neethu and Govind constructed a sodium alginate-GO-chitosan drug carrier system and loaded it with amoxicillin.<sup>87</sup> The novel drug molecule showed a controlled release with high sensitivity against *Staphylococcus aureus* and *Escherichia coli*, with 13 mm and 30 mm diameter zones of inhibition for *Staphylococcus aureus* and *Escherichia coli*, respectively. The novel drug molecule also showed high cell viability towards a mouse fibroblast cell line with 99.71% viability. This composite exemplifies how GO can be integrated synergistically with biopolymers to balance efficacy and biocompatibility.

Pulingam *et al.*<sup>98</sup> reported the synergetic antibacterial activity of GO and antibiotics when they tested 10  $\mu\text{g mL}^{-1}$  GO with varying concentrations (1–10  $\mu\text{g mL}^{-1}$ ) of chloramphenicol, ampicillin, and tetracycline against *Staphylococcus aureus*, *Enterococcus faecalis*, *Escherichia coli*, and *Pseudomonas aeruginosa*. The combination exhibited significant synergistic antibacterial activity against all bacterial groups, with higher activity observed in the Gram-positive bacteria compared to the Gram-negative bacteria. *Pseudomonas aeruginosa* showed the lowest antibacterial activity. To assess the synergetic effect of GO and Vancomycin on Vancomycin-Resistant *Staphylococcus aureus*, broth dilution and disc diffusion assays were carried out. Broth dilution results and cell viability of bacterial cells demonstrated a higher antibacterial activity of GO-Vancomycin compared to Vancomycin and GO alone. Increasing the concentration of GO-Vancomycin eradicated the bacteria. The results for zones of inhibition for GO-Vancomycin and vancomycin were 20 mm and 9 mm in diameter, respectively, while GO showed no zone of inhibition against *Staphylococcus aureus*.<sup>99</sup>

GO-gelatin-Meropenem (GO-Gel-Mer) conjugate demonstrated synergistic antibacterial activity of 45–50% higher than Meropenem alone when tested against *Staphylococcus aureus*, *Escherichia coli*, *Listeria monocytogenes*, and *Salmonella typhimurium*.<sup>100</sup> The inhibition zones for Meropenem alone were 9 mm against *Escherichia coli*, and 6 mm against *Listeria monocytogenes*, *Staphylococcus aureus*, and *Salmonella typhimurium*, while GO-Gel-Mer exhibited improved antibacterial activity with zones of inhibition of 17 mm, 11 mm, 10 mm, and 12 mm against *Escherichia coli*, *Listeria monocytogenes*, *Staphylococcus aureus*, and *Salmonella typhimurium*, respectively.<sup>100</sup>

In another study involving GO and Meropenem, the antibacterial activity of GO, Meropenem, and GO-Meropenem revealed that GO-Meropenem possessed synergetic and additive antibacterial effects against *Pseudomonas aeruginosa*, *Acinetobacter bau-*

*mannii*, *Escherichia coli*, and *Klebsiella pneumoniae*. The fractional inhibitory concentration (FIC) value of 0.37 indicated a synergistic effect for *Acinetobacter baumannii*, whereas *Pseudomonas aeruginosa*, *Escherichia coli*, and *Klebsiella pneumoniae* showed additive effects with FIC values between 0.62 and 0.75. The minimum inhibitory concentration for GO-Meropenem was lower (4–16  $\mu\text{g mL}^{-1}$ ) than GO and Meropenem alone, with 8–128  $\mu\text{g mL}^{-1}$  and 32–128  $\mu\text{g mL}^{-1}$ , respectively.<sup>101</sup> Key literature examples demonstrating GO-antibiotic synergy across multiple drug classes and bacterial models are consolidated in Fig. 9.

Worth knowing is that not all GO-antibiotic combinations result in synergistic antibacterial effects. Gao *et al.* studied the combined antibacterial action of GO with Lincomycin hydrochloride (LMH), Chloramphenicol (CPC), and Gentamicin sulfate (GMS) against *Escherichia coli* and *Staphylococcus aureus*. Against *Escherichia coli*, LMH alone produced about 20% inhibition at 20  $\text{mg L}^{-1}$  and 80% inhibition at 1  $\text{mg L}^{-1}$  LMH and 10  $\text{mg L}^{-1}$  GO.<sup>102</sup> In contrast, the antibacterial effect of CPC on *Escherichia coli* increased with increasing CPC concentration but decreased upon the addition of 10  $\text{mg L}^{-1}$  GO. This reduction was attributed to strong  $\pi$ - $\pi$  interactions between CPC and GO, which boosted GO aggregation, limited drug release, and reduced membrane damage. GMS inhibited *Escherichia coli* by more than 95% at all tested dosages; however, when mixed with GO, its efficiency diminished due to adsorption and reduced bioavailability. Against *Staphylococcus aureus*, GO enhanced LMH activity across all concentrations tested. CPC alone showed concentration-dependent effects, and enhanced *Staphylococcus aureus* inhibition at CPC concentrations below 5  $\text{mg L}^{-1}$  with 10  $\text{mg L}^{-1}$ , but reduced *Staphylococcus aureus* at CPC concentrations above 10  $\text{mg L}^{-1}$  and 10  $\text{mg L}^{-1}$  due to increased GO aggregation. GMS showed a general decrease in antibacterial performance when combined with GO against *Staphylococcus aureus*. Additionally, the order of component addition significantly influenced antibacterial outcomes. Pre-exposure of bacteria to GO enhanced antibiotic efficacy by creating active adsorption sites and inducing membrane damage, whereas pre-mixing antibiotics with GO reduced antibiotic transport to bacterial cells, thereby lowering antibacterial effectiveness.<sup>103</sup>

Similarly, You *et al.*'s recent studies reported that GO does not always show synergy and an additive effect with antibiotics. They reported that depending on the antibiotic class and biological setting, GO can antagonize or diminish antibiotic efficacy. In their study with a cyanobacterium model (*Synechocystis* sp. PCC 6803), GO had additive effects with florfenicol but antagonistic interactions with erythromycin, ofloxacin, and chlorotetracycline due to strong antibiotic adsorption on GO, which reduced their bioavailability and biological activity.<sup>104</sup>

Because GO can also reduce antibiotic efficacy through strong adsorption, aggregation, and protocol-dependent effects (*e.g.*, order of addition), representative antagonistic/variable outcomes and formulation-dependent performance are summarized in Fig. 10.

Therefore, in the GO-antibiotic system, the degree of adsorption and bonding between GO and the antibiotic molecule, influ-



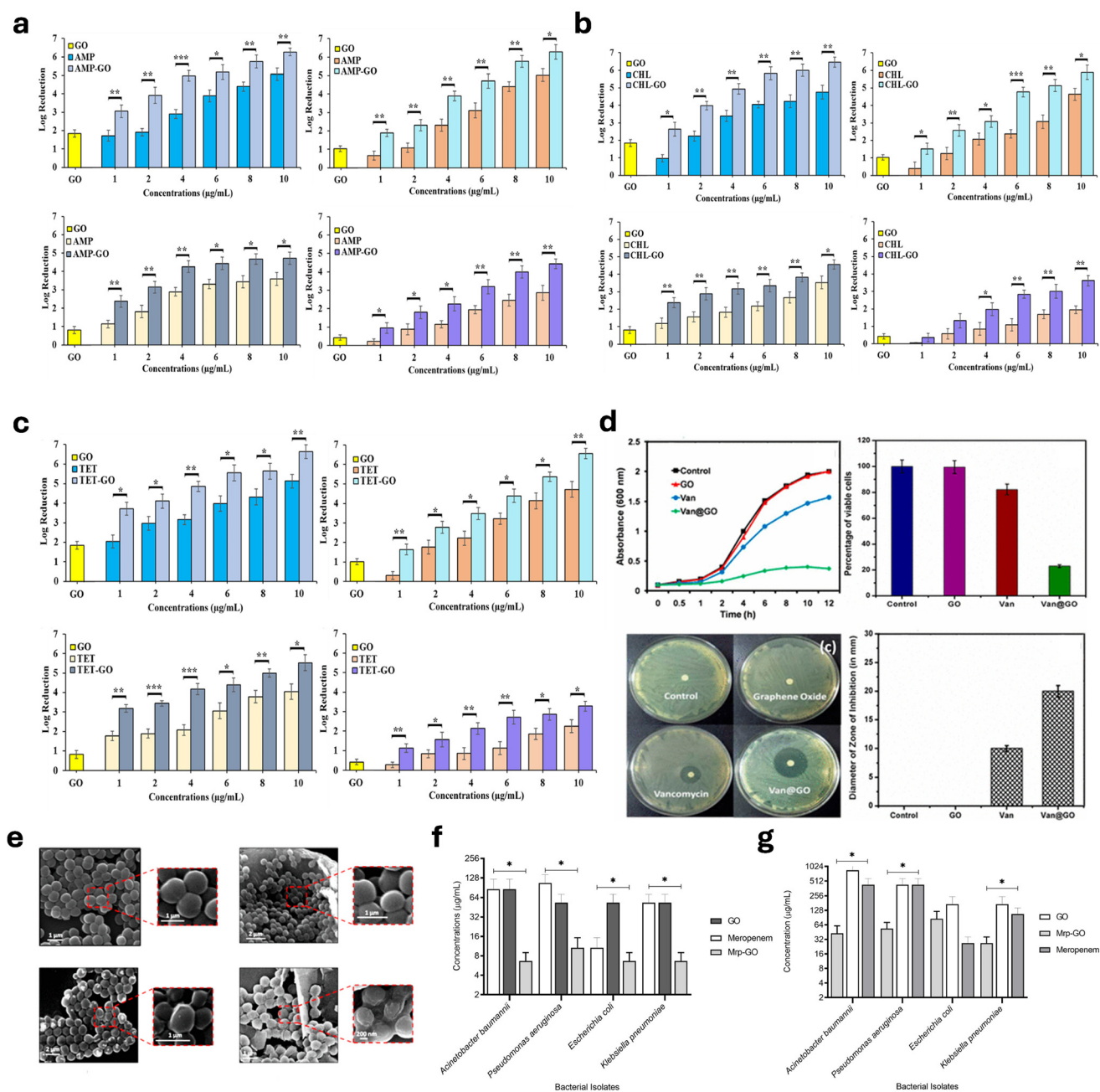


**Fig. 9** Synergistic GO-antibiotic combinations that improve antibacterial and antibiofilm effects across pathogens are exemplified. (a)–(c) Log reduction of *S. aureus*, *E. faecalis*, *E. coli*, and *P. aeruginosa* after treatment with GO ( $10 \mu\text{g mL}^{-1}$ ) and antibiotic-GO combinations: (a) AMP vs. AMP-GO, (b) CHL vs. CHL-GO, and (c) TET vs. TET-GO (mean  $\pm$  SD; significance as indicated vs. antibiotic-only). Adapted from ref. 91, Copyright 2020 Elsevier. (d) and (e) Enhanced activity of vancomycin-loaded GO (Van@GO) against VRSA: (d) OD<sub>600</sub>, CFU viability (%), inhibition-zone images, and zone diameter; (e) SEM micrographs showing VRSA morphology/interaction under control and after exposure to GO, vancomycin, and Van@GO. Adapted from ref. 99, Copyright 2019 American Chemical Society. (f) and (g) Antibacterial and antibiofilm effects of meropenem-loaded GO (Mrp-GO) compared with free meropenem (Mrp) and GO. Adapted from ref. 101, Copyright 2023 Elsevier.

enced by the antibiotic chemistry and the type of bacterial strain, determines whether the combined effect would be synergistic, additive, or antagonistic. Hence, the need for evaluating GO-antibiotic combinations on an individual or class of antibiotics basis. The antibacterial effects of GO-antibiotics against different antibiotic-resistant bacteria are presented in Table 3.

## 5. Challenges and limitations of GO as a nanocarrier

GO as a nanocarrier faces challenges and limitations, especially regarding its stability, biocompatibility, scalability, and commercial viability. The obstacles are not exclusively for-



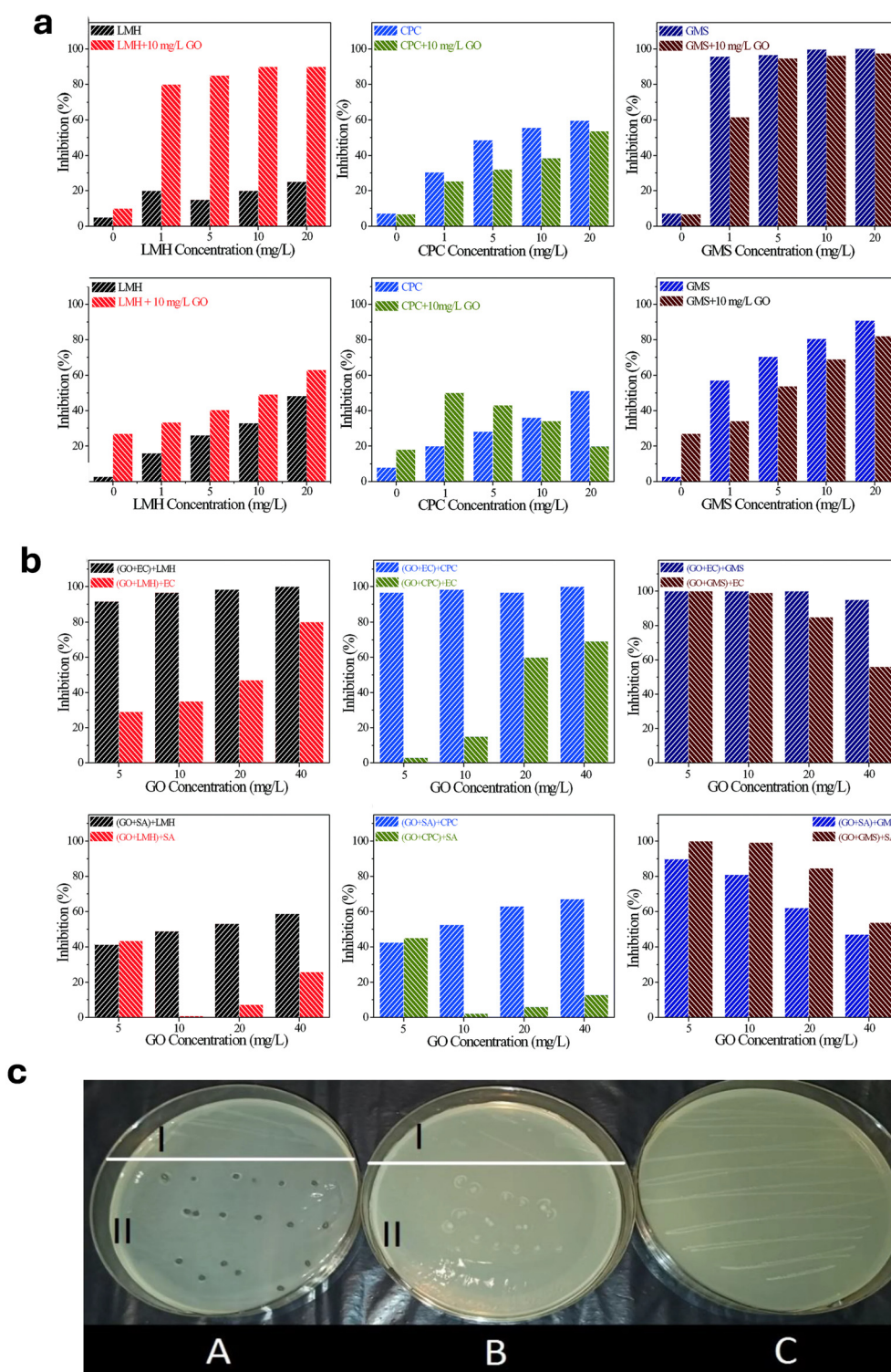


**Fig. 10** Evidence of antagonism in GO-antibiotic synergy systems: adsorption/aggregation and order-of-addition effects on antibacterial inhibition. (a) and (b) Impact of GO on antibiotic efficacy against *E. coli* and *S. aureus*: (a) growth inhibition after exposure to LMH, CPC, and GMS in the absence and presence of GO ( $10 \text{ mg L}^{-1}$ ); (b) growth inhibition as a function of order of addition (antibiotic =  $10 \text{ mg L}^{-1}$ ; EC = *E. coli*, SA = *S. aureus*). Adapted from ref. 103, Copyright 2017 Royal Society of Chemistry. (c) Growth inhibition of *E. faecalis* under amoxicillin (AMOX) release conditions comparing (A) GO-AMOX + bromelain (BROM) alginate capsules, (B) AMOX-only alginate capsules, and (C) control ( $37 \text{ }^\circ\text{C}$ , 72 h). Adapted from ref. 45, Copyright 2021 MDPI.



**Table 3** Antibacterial activity of GO-antibiotics

Bacteria tested	Antibiotics used with GO	Results	Ref.
<i>Staphylococcus aureus</i> , <i>Escherichia coli</i>	Amoxicillin	30 mm and 13 mm diameter zones of inhibition for <i>Staphylococcus aureus</i> , <i>Escherichia coli</i>	87
<i>Enterococcus faecalis</i>	Amoxicillin	Enzyme-controlled release of amoxicillin from hydrogel effectively inhibited the growth of the <i>Enterococcus faecalis</i> strain	45
<i>Enterococcus faecalis</i>	Ciprofloxacin and Metronidazole (DAP)	GO-DAP completely eradicated <i>Enterococcus faecalis</i> within 24 hours and eliminated a significantly greater bacterial count than DAP and GO alone during the experiment	32
<i>Staphylococcus aureus</i> , <i>Enterococcus faecalis</i> , <i>Escherichia coli</i> , and <i>Pseudomonas aeruginosa</i>	Chloramphenicol, Ampicillin, and Tetracycline	The combination showed significant synergetic antibacterial activity in all bacterial groups	98
<i>Escherichia coli</i> and <i>Staphylococcus aureus</i>	Lincomycin hydrochloride, Chloramphenicol, and Gentamicin sulfate	Increased antibacterial activity for GO-LMH but a reduction in antibacterial efficacy for GO-CPC and GO-GMS	103
<i>Escherichia coli</i> , <i>Listeria monocytogenes</i> , <i>Staphylococcus aureus</i> , and <i>Salmonella typhimurium</i>	Meropenem	GO-gelatin-Meropenem (GO-Gel-Mer) conjugate demonstrated synergistic antibacterial activity of 45–50% higher than Meropenem alone when tested against <i>Staphylococcus aureus</i> , <i>Escherichia coli</i> , <i>Listeria monocytogenes</i> , and <i>Salmonella typhimurium</i>	100
<i>Pseudomonas aeruginosa</i> , <i>Acinetobacter baumannii</i> , <i>Escherichia coli</i> , and <i>Klebsiella pneumoniae</i> .	Meropenem	The minimum inhibitory concentration for GO-Meropenem was lower ( $4\text{--}16\ \mu\text{g mL}^{-1}$ ) than GO and Meropenem alone with $8\text{--}128\ \mu\text{g mL}^{-1}$ and $32\text{--}128\ \mu\text{g mL}^{-1}$ respectively	101
<i>Staphylococcus aureus</i>	Vancomycin	The results for zones of inhibition for GO-Vancomycin and vancomycin were 20 mm and 9 mm in diameter respectively while GO showed no zone of inhibition against <i>Staphylococcus aureus</i>	99

mulation issues but also host biological reactions, pharmacokinetics, long-term safety, and regulatory feasibility, all of which must be addressed for the clinical translation of GO as an antibiotic carrier.<sup>52</sup> This section delves into the challenges and limitations of GO as a nanocarrier of drug molecules (Fig. 11).

### 5.1. Chemical Instability

The practical use of GO-based systems depends on system stability, but this requirement remains a significant technical challenge. GO shows intrinsic instability in aqueous solutions due to its structural and interaction properties, which prevent consistent formulation performance. The chemical structure of GO is sensitive to aqueous conditions, leading to structural degradation and a subsequent decrease in its functional properties. The water-loving properties of GO, combined with its tendency to clump, are the primary cause of instability when the material is present in aqueous solutions.<sup>105</sup> These effects can lead to variable antibiotic release and diminished efficacy. This inconsistency is further confounded by the absence of standardized formulation and characterization procedures across studies, which makes it challenging to assess and compare stability and performance profiles. Also, instability in biological fluids, especially in the presence of salts and proteins, may increase aggregation and affect repeatability *in vivo*.<sup>30</sup>

The chemical characteristics of GO, particularly its oxygen-containing functional groups, can affect the stability of the resulting formulations, requiring thorough supervision and modification to improve stability.<sup>106</sup> The membrane stability of

GO depends on both structural design and proper engineering of surfaces and interfaces.<sup>107</sup> However, the stability of GO-based nanocarriers can be enhanced through cross-linking with molecules or ions while using mixed materials in the formulations. The introduction of intermolecular bonds through hydrogen interactions strengthens the bond between GO layers and substrates, improving structural stability.<sup>106</sup> However, careful optimization is necessary as excessive modification may influence antibiotic-loading capacity and biocompatibility.

Like other nanoparticle systems, GO formulations are prone to aggregation due to elevated surface energy, resulting in sedimentation and diminished stability over time.<sup>108</sup> Stabilizers, including polymers and surfactants, are frequently employed to inhibit aggregation *via* electrostatic repulsion or steric hindrance; however, their efficacy may differ based on the formulation.<sup>109</sup> As aggregation may reduce the effective surface area of GO, limit antibiotic adsorption efficiency, influence biodistribution by altering circulation time, and affect antimicrobial activity,<sup>30</sup> Therefore, mitigation of aggregation in GO-based delivery systems is a barrier that must be addressed.

### 5.2. Biocompatibility, biodistribution, and clearance

When GO is administered intravenously to mice, biodistribution studies show that it predominantly accumulates in the lungs, liver, and spleen, with smaller quantities found in the bone, heart, and brain. This organ distribution is typical of many nanomaterials and reflects uptake by the reticuloendothelial system (RES), which can limit effective delivery to



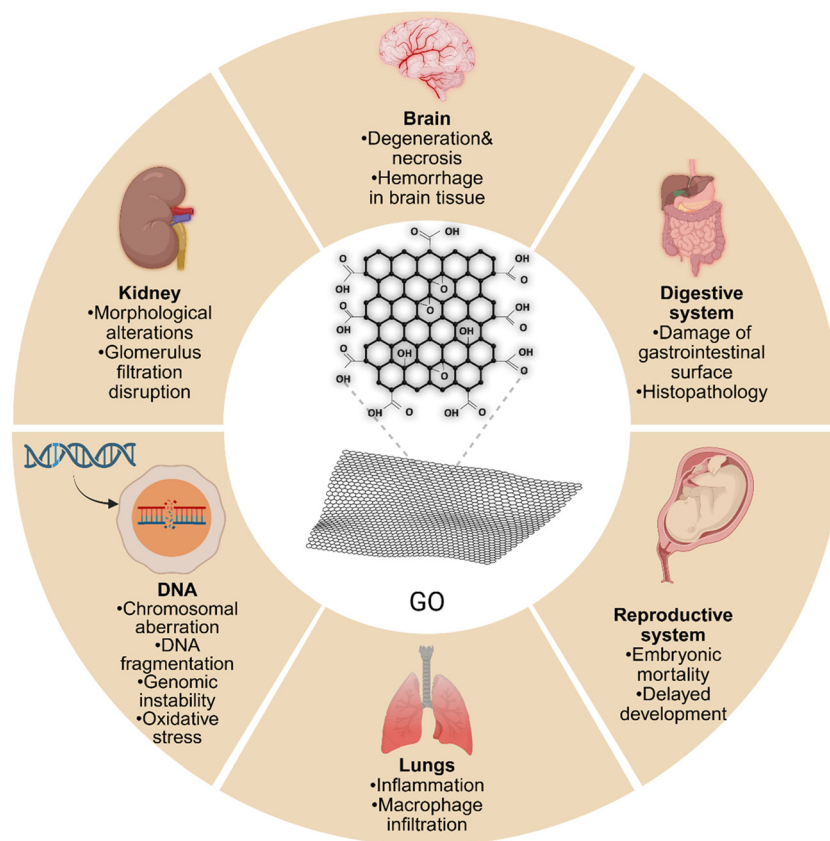


Fig. 11 The harmful effects of high-concentration GO in major organs of the human body.

infection sites.<sup>110,111</sup> Oxidative stress, apoptosis, and genotoxicity have been observed in cells exposed to GO. However, studies report no significant changes in cell shape, viability, or membrane integrity at lower doses. Thus, current data findings indicate that GO exhibits biocompatibility at low concentrations but may raise safety concerns at higher concentrations and prolonged exposure.<sup>14</sup> Importantly, immune system activation, complement activation, and cytokine release have been observed in some *in vivo* studies, indicating potential immunotoxicity that depends on surface chemistry and dose.<sup>112</sup> Furthermore, longitudinal studies have shown that incomplete clearance and prolonged tissue retention of GO can lead to persistent inflammation, fibrotic responses, and altered organ function, highlighting the need to understand degradation pathways and excretion mechanisms.<sup>113</sup> In this context, reported 'biodegradation' of GO should be interpreted primarily as immune-linked oxidative biotransformation (structural oxidation or fragmentation) under specific inflammatory or peroxidase-rich conditions, rather than universal rapid elimination. Clearance is likewise formulation-dependent: larger or RES-associated GO fractions are more plausibly processed *via* hepatic handling and hepatobiliary elimination, whereas renal excretion is more feasible only for sufficiently small and well-dispersed fractions. Therefore, biodegradability and excretion should be framed as conditional properties requiring long-

term *in vivo* quantification.<sup>114</sup> However, most available biocompatibility data are derived from *in vitro* models or short-term animal studies, while systematic long-term *in vivo* toxicity and biodegradation data remain limited, and therefore require comprehensive long-term studies involving human subjects to confirm these findings. One of the most challenging issues in developing GO-based medication delivery systems is regulating potential toxicity and understanding the degradation and excretion mechanisms in living organisms. Surface modifications for functional applications and degradation ability represent the best option for successfully utilizing GO in biomedical applications.<sup>115</sup> GO's unique structure, drug-loading capabilities, and its great potential for use as a drug carrier and other clinical applications require improvements in toxicity issues, alongside better biocompatibility results, and safe degradation solutions through surface modification with biocompatible polymers. These modifications improve GO circulation time and reduce immune system recognition.<sup>115</sup> However, extended circulation may increase tissue accumulation, indicating a significant trade-off between pharmacokinetics and long-term safety, which must be carefully optimized.<sup>116</sup>

### 5.3. Ethical Implications

GO possesses potential legal barriers in its use as a nano-carrier platform, particularly in biological applications. These



barriers are primarily regulatory and safety-related rather than legal in a conventional sense and stem from uncertainties surrounding the biological fate, toxicity, and environmental impact of GO. The major difficulties emerge from health dangers that arise from nano-matter exposure and ethical operational choices. Thus, ethical issues are essential for guaranteeing safe and responsible advancement and application of GO-based technology.<sup>117</sup> These considerations, including patient safety, informed consent, and environmental responsibility, must be addressed.

On occupational exposure, there is insufficient scientific clarification concerning the health implications of workplace exposure to nanoparticles, especially GO. This includes uncertainty regarding safe exposure limits during GO synthesis, processing, and handling, as well as the lack of GO-specific occupational safety guidelines. This ambiguity requires ethical decision-making to safeguard workers from possible dangers.<sup>118</sup> GO may accumulate in tissues, potentially eliciting toxic reactions and delicate inflammatory responses. This is particularly essential due to the varied side-effects of GO that have been reported to depend strongly on GO dose, lateral sheet size, surface chemistry, and aggregation state. These outcomes generate ethical issues regarding the safety and long-term health consequences for those exposed to GO-based nanocarriers.<sup>119,120</sup> The absence of a standard protocol for the synthesis, characterization, and biological applications of GO nanomaterials is a significant limitation in this field. Lack of standard procedures for the characterization of GO, including size, thickness, degree of oxidation, surface charge, and dispersion stability, is a critical limitation for reproducibility, toxicity comparisons, and clinical translation.

Furthermore, a lack of standardized antibacterial methods, including differences in inoculum size, antibacterial assay (*e.g.*, MIC, disk diffusion, time-kill), and reporting methods (activity index, inhibition zone, and growth percentage), also limits the comparability of studies and results in variation in the conclusions about antibacterial properties. Also, limited biodegradability experimental results of GO raise concerns regarding the environmental persistence of GO following large-scale biomedical or industrial use. Collectively, these factors highlight the need for GO-specific regulatory frameworks and risk assessment strategies to enable the safe translation of GO-based antibiotic delivery systems from laboratory research to clinical and environmental settings.

#### 5.4. Scalability and Commercial Viability

GO has substantial capacity as a nanocarrier because of its distinctive features; however, its commercial viability and scalability are hindered by numerous obstacles. The complexities of its production, the necessity for consistent quality, and the economic feasibility of large-scale manufacturing are the sources of these challenges. The full potential of GO in commercial applications must be realized by overcoming the technical and economic obstacles that arise during the transition from laboratory-scale synthesis to industrial-scale production.<sup>120</sup> The scalability of GO production is hindered by

difficulties in producing ultra-large GO (ULGO), primarily due to sheet fragmentation and gelation. Thus, it is challenging to maintain the structural integrity of GO sheets during the oxidation and purification procedures.<sup>120</sup> Also, choosing the appropriate starting material and reaction media constitutes an essential factor for obtaining GO. Production costs remain a key challenge, as the reaction depends on the oxidation process.<sup>121</sup> Furthermore, it is challenging to obtain consistent product quality, resulting in batch-to-batch variations. This is part of the larger lack of standardized manufacturing and quality control processes for GO, which is a major obstacle to scaling up and regulatory approval.<sup>122</sup> The quality assessment of GO requires strict protocols that add resources and expense to production costs.<sup>121</sup>

Finally, the synthesis of GO generates significant amounts of wastewater, requiring specialized treatment methods for environmentally responsible disposal. Additionally, without more efficient production routes, high costs are likely to prevent widespread adoption and commercialization.<sup>121</sup> In general, the absence of standardized protocols for the synthesis, characterization, biological testing, and reporting is a key challenge in the field, and limits the reproducibility, inter-study comparison, and translation to clinical practice of GO-based antibiotic delivery systems. Addressing these challenges will be critical for translating GO-based technologies from research to market applications.

## 6. Future directions and prospectives

The formulation techniques for GO alongside antibiotics establish promising outcomes through enhanced antibiotic effect and delivery precision. GO is a promising candidate for drug delivery, undergoing scientific investigation due to its distinctive functional properties and high surface area. Recent studies have prioritized both GO-based nanosheet development alongside antibiotic integration to fight microorganisms that have become drug-resistant. These developments have been created to improve treatment effectiveness through better drug capacity, antimicrobial properties, and release kinetics control. Thus, modern advancements in technology stimulate medical research to achieve better treatment outcomes, address antibiotic resistance with better drugs, and improve delivery systems. The objective of these advancements is to enhance therapeutic outcomes and address the challenges of antibiotic resistance by enhancing drug loading efficiency, release profiles, and antimicrobial activity.<sup>96</sup> Paramount among innovative GO formulations for better antibacterial efficacy is the integration of other materials. Scientific analysis is investigating the integration of GO with multiple materials, including biodegradable polymers and nanocarriers, to develop more extended-release properties for antibiotics. The approach targets maintaining drug levels above the MIC (minimum inhibitory concentration) to reduce resistance development in bacteria for long-duration applications.<sup>123,124</sup> In combination therapy, researchers have achieved success in



using GO to deliver multiple drugs. Thus, future research on multiple-antibiotic delivery *via* GO for managing multidrug-resistant bacteria is needed.<sup>3</sup>

## 7. Conclusion

GO has emerged as a game-changing nanocarrier for antibiotic delivery, combining unparalleled potential with its high surface area, biocompatibility, and versatile functionalization capabilities. Beyond enhancing antibiotic efficacy, GO precisely targets multidrug-resistant bacteria, opening the door to a broader range of treatment options. Its advanced drug-delivery features, controlled release, antibacterial activity, and synergy with combination therapies make it a leader in combating bacterial resistance. However, challenges like chemical instability, aggregation, potential toxicity, and scalability pose hurdles to its clinical breakthrough. To utilize GO's full potential, several steps should be considered, including conducting more *in vivo* and *in vitro* studies and environmental assessments. Furthermore, careful standardization, safety evaluation, and regulatory oversight are required to advance GO-based antibiotic delivery systems toward widespread clinical adoption and to make GO a more prominent agent in the fight against antimicrobial diseases by reducing the incidence of antibiotic resistance.

## Author contributions

Mark Dakurah and Hasibul Islam were involved in the original draft, data curation, software development, figure preparation, table preparation, and conceptualization. Khandoker Asiqur Rahaman is involved in reviewing, graphical design, and editing the original draft. Nadeem Baig is involved in reviewing and editing the original draft. Shihab Uddin is involved in conceptualization, review, and editing of the original draft writing manuscript, supervision, project administration, and resource management.

## Conflicts of interest

The authors assert that they don't have any identifiable conflicts.

## Data availability

No data was used for the research described in the article.

## Acknowledgements

This research was funded by the Interdisciplinary Research Center for Bio Systems and Machines, King Fahd University of

Petroleum & Minerals, 31261, Dhahran, Saudi Arabia (Fund Number INBS2606).

## References

- 1 M. T. H. Aunkor, T. Raihan, S. H. Prodhon, H. S. C. Metselaar, S. U. F. Malik and A. K. Azad, *R. Soc. Open Sci.*, 2020, **7**, 200640, DOI: [10.1098/rsos.200640](https://doi.org/10.1098/rsos.200640).
- 2 C. I. Colino, J. M. Lanao and C. Gutierrez-Millan, *Mater. Sci. Eng., C*, 2021, **121**, 111843, DOI: [10.1016/j.msec.2020.111843](https://doi.org/10.1016/j.msec.2020.111843).
- 3 A. León-Buitimea, C. R. Garza-Cárdenas, M. F. Román-García, C. A. Ramírez-Díaz, M. Ulloa-Ramírez and J. R. Morones-Ramírez, *Antibiotics*, 2022, **11**, 794, DOI: [10.3390/antibiotics11060794](https://doi.org/10.3390/antibiotics11060794).
- 4 H. Zheng, Z. Ji, K. R. Roy, M. Gao, Y. Pan, X. Cai, L. Wang, W. Li, C. H. Chang, C. Kaweeteerawat, C. Chen, T. Xia, Y. Zhao and R. Li, *ACS Nano*, 2019, **13**(10), 11488–11499, DOI: [10.1021/acsnano.9b04970](https://doi.org/10.1021/acsnano.9b04970).
- 5 D. R. Evans, M. P. Griffith, A. J. Sundermann, K. A. Shutt, M. I. Saul, M. M. Mustapha, J. W. Marsh, V. S. Cooper, L. H. Harrison and D. Van Tyne, *eLife*, 2020, **9**, e53886, DOI: [10.7554/eLife.53886](https://doi.org/10.7554/eLife.53886).
- 6 I. Sengupta, S. S. S. Sharat Kumar, K. Gupta and S. Chakraborty, *Mater. Today Commun.*, 2021, **26**, 101737, DOI: [10.1016/j.mtcomm.2020.101737](https://doi.org/10.1016/j.mtcomm.2020.101737).
- 7 F. A. Al-Wrafy, A. A. Al-Gheethi, S. K. Ponnusamy, E. A. Noman and S. A. Fattah, *Chemosphere*, 2022, **288**, 132603, DOI: [10.1016/j.chemosphere.2021.132603](https://doi.org/10.1016/j.chemosphere.2021.132603).
- 8 R. Solanki, N. Makwana, R. Kumar, M. Joshi, A. Patel, D. Bhatia and D. K. Sahoo, *RSC Adv.*, 2024, **14**, 33568, DOI: [10.1039/d4ra06117a](https://doi.org/10.1039/d4ra06117a).
- 9 C. Wang, Y. Yang, Y. Cao, K. Liu, H. Shi, X. Guo, W. Liu, R. Hao, H. Song and R. Zhao, *Biomater. Sci.*, 2022, **11**, 432–444, DOI: [10.1039/d2bm01489k](https://doi.org/10.1039/d2bm01489k).
- 10 F. Perreault, A. F. De Faria, S. Nejati and M. Elimelech, *ACS Nano*, 2015, **9**, 7226–7236, DOI: [10.1021/acsnano.5b02067](https://doi.org/10.1021/acsnano.5b02067).
- 11 R. Darini, H. Ahari, A. Khosrojerdi, *et al.*, *Sci. Rep.*, 2025, **15**, 1007, DOI: [10.1038/s41598-024-84335-x](https://doi.org/10.1038/s41598-024-84335-x).
- 12 M. K. Purkait, A. D. Sontakke and Anweshan, *Carbon-Based Nanocarriers for Drug Delivery*, 2023, 348, DOI: [10.1201/9781003358114](https://doi.org/10.1201/9781003358114).
- 13 S. Su, J. Wang, J. Qiu, R. Martinez-Zaguilan, S. R. Sennoune and S. Wang, *Mater. Sci. Eng., C*, 2020, **107**, 110313, DOI: [10.1016/j.msec.2019.110313](https://doi.org/10.1016/j.msec.2019.110313).
- 14 I. M. J. Ng and S. Shamsi, *Int. J. Mol. Sci.*, 2022, **23**, 9096, DOI: [10.3390/ijms23169096](https://doi.org/10.3390/ijms23169096).
- 15 R. Kumar, M. Kumar, A. Kumar, R. Singh, R. Kashyap, S. Rani and D. Kumar, Surface Modification of Graphene Oxide Using Esterification, *Mater. Today: Proc.*, 2019, **18**, 1556–1561, DOI: [10.1016/j.matpr.2019.06.626](https://doi.org/10.1016/j.matpr.2019.06.626).
- 16 O. Akhavan and E. Ghaderi, *ACS Nano*, 2010, **4**, 5731–5736, DOI: [10.1021/nn101390x](https://doi.org/10.1021/nn101390x).



- 17 S. Gurunathan, J. W. Han, A. A. Dayem, V. Eppakayala and J. H. Kim, *Int. J. Nanomed.*, 2012, **7**, 5901–5914, DOI: [10.2147/IJN.S37397](https://doi.org/10.2147/IJN.S37397).
- 18 H. Ji, H. Sun and X. Qu, *Adv. Drug Delivery Rev.*, 2016, **105**, 176–189, DOI: [10.1016/j.addr.2016.04.009](https://doi.org/10.1016/j.addr.2016.04.009).
- 19 X. M. Han, K. W. Zheng, R. L. Wang, S. F. Yue, J. Chen, Z. W. Zhao, F. Song, Y. Su and Q. Ma, *Am. J. Transl. Res.*, 2020, **12**(5), 1515–1534.
- 20 R. Muñoz, D. P. Singh, R. Kumar and A. Matsuda, in *Nanostructured Polymer Composites for Biomedical Applications*, ed. S. K. Swain and M. Jawaid, 2019, ch. 22, pp. 447–488. DOI: [10.1016/B978-0-12-816771-7.00023-5](https://doi.org/10.1016/B978-0-12-816771-7.00023-5).
- 21 M. Hoseini-Ghahfarokhi, S. Mirkiani, N. Mozaffari, M. A. A. Sadatlu, A. Ghasemi, S. Abbaspour, M. Akbarian, F. Farjadian and M. Karimi, *Int. J. Nanomed.*, 2020, **15**, 9469–9496, DOI: [10.2147/IJN.S265876](https://doi.org/10.2147/IJN.S265876).
- 22 S. Liu, M. Hu, T. H. Zeng, R. Wu, R. Jiang, J. Wei, L. Wang, J. Kong and Y. Chen, *Langmuir*, 2012, **28**, 12364–12372, DOI: [10.1021/la3023908](https://doi.org/10.1021/la3023908).
- 23 X. Lu, X. Feng, J. R. Werber, C. Chu, I. Zucker, J. H. Kim, C. O. Osuji and M. Elimelech, *Proc. Natl. Acad. Sci. U. S. A.*, 2017, **114**(46), E9793–E9801, DOI: [10.1073/pnas.1710996114](https://doi.org/10.1073/pnas.1710996114).
- 24 M. Y. Xia, Y. Xie, C. H. Yu, G. Y. Chen, Y. H. Li, T. Zhang and Q. Peng, *J. Controlled Release*, 2019, **307**(10), 16–31, DOI: [10.1016/j.jconrel.2019.06.011](https://doi.org/10.1016/j.jconrel.2019.06.011).
- 25 C. H. Yu, G. Y. Chen, M. Y. Xia, Y. Xie, Y. Q. Chi, Z. Y. He, C. L. Zhang, T. Zhang, Q. M. Chen and Q. Peng, *Colloids Surf., B*, 2020, **191**, 111009, DOI: [10.1016/j.colsurfb.2020.111009](https://doi.org/10.1016/j.colsurfb.2020.111009).
- 26 T. T. V. Truong, S. R. Kumar, Y. T. Huang, D. W. Chen, Y. K. Liu and S. J. Lue, *Nanomaterials*, 2020, **10**, 1207, DOI: [10.3390/nano10061207](https://doi.org/10.3390/nano10061207).
- 27 V. Ravikumar, I. Mijakovic and S. Pandit, *Int. J. Nanomed.*, 2022, **17**, 6707–6721, DOI: [10.2147/IJN.S387590](https://doi.org/10.2147/IJN.S387590).
- 28 M. F. Gilsanz-Muñoz, M. Martínez-Martínez, J. Pérez-Piñero, M. Roldán, M. P. Arce, R. Blasco, L. R. Román, F. Esperón-Fajardo, A. Cerpa-Naranjo and B. Martín-Maldonado, *Sci*, 2024, **6**, 66, DOI: [10.3390/sci6040066](https://doi.org/10.3390/sci6040066).
- 29 X. Huang, W. Zhao, F. Khalilov and N. Xu, *Materials*, 2025, **18**, 2855, DOI: [10.3390/ma18122855](https://doi.org/10.3390/ma18122855).
- 30 E. Quagliarini, D. Pozzi, F. Cardarelli and G. Caracciolo, *J. Nanobiotechnol.*, 2023, **21**, 267, DOI: [10.1186/s12951-023-02030-x](https://doi.org/10.1186/s12951-023-02030-x).
- 31 C. Si, Z. Sun and F. Liu, *Nanoscale*, 2016, **8**, 3207–3217, DOI: [10.1039/C5NR07755A](https://doi.org/10.1039/C5NR07755A).
- 32 F. Eskandari, A. Abbaszadegan, A. Gholami and Y. Ghahramani, *BMC Oral Health*, 2023, **23**, 20, DOI: [10.1186/s12903-023-02718-4](https://doi.org/10.1186/s12903-023-02718-4).
- 33 A. Jiříčková, O. Jankovský, Z. Sofer and D. Sedmidubský, *Materials*, 2022, **15**, 920, DOI: [10.3390/ma15030920](https://doi.org/10.3390/ma15030920).
- 34 Z. Guo, S. Chakraborty, F. A. Monikh, D. D. Varsou, A. J. Chetwynd, A. Afantitis, I. Lynch and P. Zhang, *Adv. Biol.*, 2021, **5**, e2100637, DOI: [10.1002/adbi.202100637](https://doi.org/10.1002/adbi.202100637).
- 35 N. P. Katuwavila, Y. Amarasekara, V. Jayaweera, C. Rajaphaksha, C. Gunasekara, I. C. Perera, G. A. J. Amaratunga and L. Weerasinghe, *J. Pharm. Sci.*, 2020, **109**, 1130–1135, DOI: [10.1016/j.xphs.2019.09.022](https://doi.org/10.1016/j.xphs.2019.09.022).
- 36 Z. Guo, S. Chakraborty, F. A. Monikh, D. D. Varsou, A. J. Chetwynd, A. Afantitis, I. Lynch and P. Zhang, *Adv. Biol.*, 2021, **5**, e2100637, DOI: [10.1002/adbi.202100637](https://doi.org/10.1002/adbi.202100637).
- 37 E. N. Zare, A. Mudhoo, M. A. Khan, *et al.*, *Environ. Chem. Lett.*, 2021, **19**, 3075–3114, DOI: [10.1007/s10311-021-01207-w](https://doi.org/10.1007/s10311-021-01207-w).
- 38 E. Demirel and Y. Y. Durmaz, *Eur. Polym. J.*, 2023, **186**, 111841, DOI: [10.1016/j.eurpolymj.2023.111841](https://doi.org/10.1016/j.eurpolymj.2023.111841).
- 39 N. T. Fard, H. A. Panahi, E. Moniri and E. R. Soltani, *J. Mol. Liq.*, 2024, **399**, 124393, DOI: [10.1016/j.molliq.2024.124393](https://doi.org/10.1016/j.molliq.2024.124393).
- 40 Y. Chang, S. T. Yang, J. H. Liu, E. Dong, Y. Wang, A. Cao, Y. Liu and H. Wang, *Toxicol. Lett.*, 2011, **200**, 201–210, DOI: [10.1016/j.toxlet.2010.11.016](https://doi.org/10.1016/j.toxlet.2010.11.016).
- 41 J. Russier, E. Treossi, A. Scarsi, F. Perrozzi, H. Dumortier, L. Ottaviano, M. Meneghetti, V. Palermo and A. Bianco, *Nanoscale*, 2013, **5**, 11234–11247, DOI: [10.1039/C3NR03543C](https://doi.org/10.1039/C3NR03543C).
- 42 X. Pei, Z. Zhu, Z. Gan, J. Chen, X. Zhang, X. Cheng, Q. Wan and J. Wang, *Sci. Rep.*, 2020, **10**, 2717, DOI: [10.1038/s41598-020-59624-w](https://doi.org/10.1038/s41598-020-59624-w).
- 43 M. M. Rahman, M. S. Islam, S. Uddin, R. Wakabayashi, M. Moniruzzaman and M. Goto, *ACS Appl. Mater. Interfaces*, 2022, **14**, 55332–55341, DOI: [10.1021/acsami.2c15636](https://doi.org/10.1021/acsami.2c15636).
- 44 A. D. Sontakke, S. Tiwari and M. K. Purkait, *FlatChem*, 2023, **38**, 100484, DOI: [10.1016/j.flatc.2023.100484](https://doi.org/10.1016/j.flatc.2023.100484).
- 45 A. Trusek and E. Kijak, *Materials*, 2021, **14**, 3182, DOI: [10.3390/ma14123182](https://doi.org/10.3390/ma14123182).
- 46 S. Uddin, M. R. Islam, M. R. Chowdhury, R. Wakabayashi, N. Kamiya, M. Moniruzzaman and M. Goto, *ACS Appl. Bio Mater.*, 2021, **4**, 6256–6267, DOI: [10.1021/acsabm.1c00563](https://doi.org/10.1021/acsabm.1c00563).
- 47 K. Shankar, S. Agarwal, S. Mishra, P. Bhatnagar, S. Siddiqui and I. Abrar, *Biomater. Adv.*, 2023, **150**, 213440, DOI: [10.1016/j.bioadv.2023.213440](https://doi.org/10.1016/j.bioadv.2023.213440).
- 48 M. Di Giulio, R. Zappacosta, S. Di Lodovico, E. Di Camppli, G. Siani, A. Fontana and L. Cellini, *Antimicrob. Agents Chemother.*, 2018, **62**, e00547–e00518, DOI: [10.1128/AAC.00547-18](https://doi.org/10.1128/AAC.00547-18).
- 49 Y. Gao, Y. Dong, Y. Cao, W. Huang, C. Yu, S. Sui, A. Mo and Q. Peng, *J. Biomed. Nanotechnol.*, 2021, **17**(8), 1627–1634, DOI: [10.1166/jbn.2021.3123](https://doi.org/10.1166/jbn.2021.3123).
- 50 S. I. Saeed, L. Vivian, C. W. S. C. W. Zalati, *et al.*, *BMC Vet. Res.*, 2023, **19**, 10, DOI: [10.1186/s12917-022-03560-6](https://doi.org/10.1186/s12917-022-03560-6).
- 51 K. AbouAitah, F. Sabbagh and B. S. Kim, *Nanomaterials*, 2023, **13**(19), 2666, DOI: [10.3390/nano13192666](https://doi.org/10.3390/nano13192666).
- 52 K. Olczak, W. Jakubowski and W. Szymański, *Materials*, 2023, **16**(11), 4199, DOI: [10.3390/ma16114199](https://doi.org/10.3390/ma16114199).
- 53 J. He, X. Zhu, Z. Qi, C. Wang, X. Mao, C. Zhu, Z. He, M. Li and Z. Tang, *ACS Appl. Mater. Interfaces*, 2015, **7**(38), 21571–21579, DOI: [10.1021/acsami.5b06876](https://doi.org/10.1021/acsami.5b06876).
- 54 M. Dallavalle, A. Bottoni, M. Calvaresi and F. Zerbetto, *ACS Appl. Mater. Interfaces*, 2018, **10**, 15487–15493, DOI: [10.1021/acsami.8b03224](https://doi.org/10.1021/acsami.8b03224).



- 55 K. Olczak, W. Jakubowski and W. Szymański, *Materials*, 2023, **16**(11), 4199, DOI: [10.3390/ma16114199](https://doi.org/10.3390/ma16114199).
- 56 W. Han, Z. Wu, Y. Li and Y. Wang, *Chem. Eng. J.*, 2019, **358**, 1022–1037, DOI: [10.1016/j.cej.2018.10.106](https://doi.org/10.1016/j.cej.2018.10.106).
- 57 F. Grilli, P. H. Gohari and S. Zou, *Int. J. Mol. Sci.*, 2022, **23**, 6802, DOI: [10.3390/ijms23126802](https://doi.org/10.3390/ijms23126802).
- 58 L. Bousiakou, R. Qindeel, O. Al-Dossary and H. Kalkani, *J. King Saud Univ., Sci.*, 2022, **34**, 102002.
- 59 X. Lu, X. Feng, J. R. Werber, C. Chu, I. Zucker, J. H. Kim, C. O. Osuji and M. Elimelech, *Proc. Natl. Acad. Sci. U. S. A.*, 2017, **114**(46), E9793–E9801, DOI: [10.1073/pnas.1710996114](https://doi.org/10.1073/pnas.1710996114).
- 60 J. Wang, Y. Wei, X. Shi and H. Gao, *RSC Adv.*, 2013, **3**, 15776–15782, DOI: [10.1039/C3RA40392K](https://doi.org/10.1039/C3RA40392K).
- 61 Y. Li, H. Yuan, A. von dem Bussche, M. Creighton, R. H. Hurt, A. B. Kane and H. Gao, *Proc. Natl. Acad. Sci. U. S. A.*, 2013, **110**(30), 12295–12300, DOI: [10.1073/pnas.1222276110](https://doi.org/10.1073/pnas.1222276110).
- 62 O. Akhavan, E. Ghaderi and A. Esfandiari, *J. Phys. Chem. B*, 2011, **115**, 6279–6288, DOI: [10.1021/jp906325q](https://doi.org/10.1021/jp906325q).
- 63 K. B. Male, A. C. W. Leung, J. Montes, A. Kamena and J. H. T. Luong, *Nanoscale*, 2012, **4**, 1373–1379, DOI: [10.1039/c2nr11886f](https://doi.org/10.1039/c2nr11886f).
- 64 A. Jimenez, F. Jaramillo, U. Hemraz, Y. Boluk, K. Ckless and R. Sunasee, *Nanotechnol., Sci. Appl.*, 2017, **10**, 123–136, DOI: [10.2147/NSA.S145891](https://doi.org/10.2147/NSA.S145891).
- 65 F. Perreault, A. F. de Faria and M. Elimelech, *Chem. Soc. Rev.*, 2015, **44**, 5861–5896, DOI: [10.1039/C5CS00021A](https://doi.org/10.1039/C5CS00021A).
- 66 V. C. Sanchez, A. Jachak, R. H. Hurt and A. B. Kane, *Chem. Res. Toxicol.*, 2012, **25**, 15–34, DOI: [10.1021/tx200339h](https://doi.org/10.1021/tx200339h).
- 67 Y. Liu, J. Wen, Y. Gao, T. Li, H. Wang, H. Yan, B. Niu and R. Guo, *Appl. Surf. Sci.*, 2024, **475**, 624–630, DOI: [10.1051/e3sconf/202447501005](https://doi.org/10.1051/e3sconf/202447501005).
- 68 Y. Qiu, Z. Wang, A. C. Owens, I. Kulaots, Y. Chen, A. B. Kane and R. H. Hurt, *Nanoscale*, 2014, **6**, 11744–11755, DOI: [10.1039/c4nr03275f](https://doi.org/10.1039/c4nr03275f).
- 69 G. Koch, A. Yepes, K. U. Förstner, C. Wermser, S. T. Stengel, J. Modamio, K. Ohlsen, K. R. Foster and D. Lopez, *Cell*, 2014, **158**, 1060–1071, DOI: [10.1016/j.cell.2014.06.046](https://doi.org/10.1016/j.cell.2014.06.046).
- 70 J. Wang, Y. Wei, X. Shi and H. Gao, *RSC Adv.*, 2013, **3**, 15776–15782, DOI: [10.1039/C3RA40392K](https://doi.org/10.1039/C3RA40392K).
- 71 S. Ma, Y. Si, F. Wang, L. Su, C. C. Xia, J. Yao, H. Chen and X. Liu, *Sci. Rep.*, 2017, **7**, 42689, DOI: [10.1038/srep42689](https://doi.org/10.1038/srep42689).
- 72 N. Bellier, P. Baipaywad, N. Ryu, J. Y. Lee and H. Park, *Biomater. Res.*, 2022, **26**, 65, DOI: [10.1186/s40824-022-00313-2](https://doi.org/10.1186/s40824-022-00313-2).
- 73 N. Karki, H. Tiwari, C. Tewari, A. Rana, N. Pandey, S. Basak and N. G. Sahoo, *J. Mater. Chem. B*, 2020, **8**, 8116–8148, DOI: [10.1039/D0TB01149E](https://doi.org/10.1039/D0TB01149E).
- 74 S. Uddin, M. R. Islam, R. Md Moshikur, R. Wakabayashi, N. Kamiya, M. Moniruzzaman and M. Goto, *ACS Appl. Bio Mater.*, 2022, **5**, 2586–2597, DOI: [10.1021/acsabm.2c00061](https://doi.org/10.1021/acsabm.2c00061).
- 75 J. Huang, D. Zhang, C. Zhu, S. Chen, Y. Wang, K. Han, S. Ci and Y. Lv, *RSC Adv.*, 2025, **15**, 26728–26738, DOI: [10.1039/d5ra01352f](https://doi.org/10.1039/d5ra01352f).
- 76 N. Mahmud, M. I. Anik, M. K. Hossain, M. I. Khan, S. Uddin, M. Ashrafuzzaman, *et al.*, *ACS Appl. Bio Mater.*, 2022, **5**, 2431–2460, DOI: [10.1021/acsabm.2c00123](https://doi.org/10.1021/acsabm.2c00123).
- 77 T. S. Anirudhan, V. Chithra Sekhar and V. S. Athira, *Int. J. Biol. Macromol.*, 2020, **150**, 468–479, DOI: [10.1016/j.ijbiomac.2020.02.053](https://doi.org/10.1016/j.ijbiomac.2020.02.053).
- 78 R. K. Layek and A. K. Nandi, *Polymer*, 2013, **54**(19), 5087–5103, DOI: [10.1016/j.polymer.2013.06.027](https://doi.org/10.1016/j.polymer.2013.06.027).
- 79 Z. Xu, S. Wang, Y. Li, M. Wang, P. Shi and X. Huang, *ACS Appl. Mater. Interfaces*, 2014, **6**, 17268–17276, DOI: [10.1021/am505308f](https://doi.org/10.1021/am505308f).
- 80 A. Yu, J. Shang, F. Cheng, B. A. Paik, J. M. Kaplan, R. B. Andrade and D. M. Ratner, *Langmuir*, 2012, **28**, 11265–11273, DOI: [10.1021/la301661x](https://doi.org/10.1021/la301661x).
- 81 P. Parsamehr, M. Zahed, M. A. Tofighy, T. Mohammadi and M. Rezakazemi, *Desalination*, 2019, **468**, 114079, DOI: [10.1016/j.desal.2019.114079](https://doi.org/10.1016/j.desal.2019.114079).
- 82 L. Tian, A. Singh and A. V. Singh, *Int. J. Biol. Macromol.*, 2020, **153**, 533–538, DOI: [10.1016/j.ijbiomac.2020.02.313](https://doi.org/10.1016/j.ijbiomac.2020.02.313).
- 83 A. Alhourani, J.-L. Førde, L. A. Eichacker, L. Herfindal and H. R. Hagland, *ACS Omega*, 2021, **6**, 24619–24629, DOI: [10.1021/acsomega.1c03283](https://doi.org/10.1021/acsomega.1c03283).
- 84 M. Colilla and M. Vallet-Regí, *Chem. Mater.*, 2023, **35**, 8788–8805, DOI: [10.1021/acs.chemmater.3c02192](https://doi.org/10.1021/acs.chemmater.3c02192).
- 85 Q. Zhou, Z. Si, K. Wang, K. Li, W. Hong, Y. Zhang and P. Li, *J. Controlled Release*, 2022, **352**, 507–526, DOI: [10.1016/j.jconrel.2022.10.038](https://doi.org/10.1016/j.jconrel.2022.10.038).
- 86 A. Ghamkhari, S. Abbaspour-Ravasjani, M. Talebi, H. Hamishehkar and M. R. Hamblin, *Int. J. Biol. Macromol.*, 2021, **169**, 521–531, DOI: [10.1016/j.ijbiomac.2020.12.084](https://doi.org/10.1016/j.ijbiomac.2020.12.084).
- 87 P. N. Das and K. G. Raj, *Int. J. Biol. Macromol.*, 2024, **254**, 127837, DOI: [10.1016/j.ijbiomac.2023.127837](https://doi.org/10.1016/j.ijbiomac.2023.127837).
- 88 A. Trusek, E. Kijak and L. Granicka, *Mater. Sci. Eng., C*, 2020, **116**, 111240, DOI: [10.1016/j.msec.2020.111240](https://doi.org/10.1016/j.msec.2020.111240).
- 89 Z. Su, D. Sun, L. Zhang, M. He, Y. Jiang, B. Millar, P. Douglas, D. Mariotti, P. Maguire and D. Sun, *Materials*, 2021, **14**, 2351, DOI: [10.3390/ma14092351](https://doi.org/10.3390/ma14092351).
- 90 M. M. Tabar, M. Khaleghi, E. Bidram, A. Zarepour and A. Zarrabi, *Pharmaceutics*, 2022, **14**, 2049, DOI: [10.3390/pharmaceutics14102049](https://doi.org/10.3390/pharmaceutics14102049).
- 91 T. Pulingam, T. Parumasivam, A. M. Gazzali, A. M. Sulaiman, J. Y. Chee, M. Lakshmanan, C. F. Chin and K. Sudesh, *Eur. J. Pharm. Sci.*, 2022, **170**, 106103, DOI: [10.1016/j.ejps.2021.106103](https://doi.org/10.1016/j.ejps.2021.106103).
- 92 G. Kumar, K. Chaudhary, N. K. Mogha, A. Kant and D. T. Masram, *ACS Omega*, 2021, **6**, 20433–20444, DOI: [10.1021/acsomega.1c02422](https://doi.org/10.1021/acsomega.1c02422).
- 93 N. Ma, A. Song, Z. Li and Y. Luan, *ACS Biomater. Sci. Eng.*, 2019, **5**(3), 1384–1391, DOI: [10.1021/acsbiomaterials.9b00114](https://doi.org/10.1021/acsbiomaterials.9b00114).
- 94 X. Huang, Z. Yin, S. Wu, X. Qi, Q. He, Q. Zhang, Q. Yan, F. Boey and H. Zhang, *Small*, 2011, **7**, 1876–1902, DOI: [10.1002/sml.201002009](https://doi.org/10.1002/sml.201002009).
- 95 D. P. Singh, C. E. Herrera, B. Singh, S. Singh, R. K. Singh and R. Kumar, *Mater. Sci. Eng., C*, 2018, **86**, 173–197, DOI: [10.1016/j.msec.2018.01.004](https://doi.org/10.1016/j.msec.2018.01.004).



- 96 A. Tiwary, B. Sapra and S. Jain, *Recent Pat. Drug Delivery Formulation*, 2008, **1**, 23–36, DOI: [10.2174/187221107779814087](https://doi.org/10.2174/187221107779814087).
- 97 P. S. Mondal, in *Proceedings of MOL2NET'22, Conference on Molecular, Biomedical, Computational and Network Science and Engineering*, MDPI, Basel, Switzerland, 8th edn, 2023. DOI: [10.3390/mol2net-08-13946](https://doi.org/10.3390/mol2net-08-13946).
- 98 T. Pulingam, K. L. Thong, J. N. Appaturi, N. I. Nordin, I. J. Dinshaw, C. W. Lai and B. F. Leo, *Eur. J. Pharm. Sci.*, 2020, **142**, 105087, DOI: [10.1016/j.ejps.2019.105087](https://doi.org/10.1016/j.ejps.2019.105087).
- 99 V. Singh, V. Kumar, S. Kashyap, A. V. Singh, V. Kishore, M. Sitti, P. S. Saxena and A. Srivastava, *ACS Appl. Bio Mater.*, 2019, **2**(3), 1148–1157, DOI: [10.1021/acsabm.8b00757](https://doi.org/10.1021/acsabm.8b00757).
- 100 M. Ranjbar, P. H. Rad, H. Rajaei Litkahi and M. Solaimani, *Int. J. Pharm.*, 2024, **666**, 124846, DOI: [10.1016/j.ijpharm.2024.124846](https://doi.org/10.1016/j.ijpharm.2024.124846).
- 101 M. Y. Memar, Y. R. Saadat, S. M. Dizaj, M. Yekani, S. M. Hejazian, B. Niknafs, S. Z. Vahed and S. Sharifi, *OpenNano*, 2023, **12**, 100155, DOI: [10.1016/j.onano.2023.100155](https://doi.org/10.1016/j.onano.2023.100155).
- 102 Y. Gao, J. Wu, X. Ren, X. Tan, T. Hayat, A. Alsaedi, C. Cheng and C. Chen, *Environ. Sci.:Nano*, 2017, **4**, 1016–1024, DOI: [10.1039/C7EN00052A](https://doi.org/10.1039/C7EN00052A).
- 103 Y. Gao, J. Wu, X. Ren, X. Tan, T. Hayat, A. Alsaedi, C. Cheng and C. Chen, *Environ. Sci. Nano*, 2017, **4**, 1016–1024, DOI: [10.1039/C7EN00052A](https://doi.org/10.1039/C7EN00052A).
- 104 M. You, X. You, X. Yang, J. Hu and W. Sun, *Environ. Sci. Nano*, 2022, **9**, 243–253, DOI: [10.1039/D1EN00763G](https://doi.org/10.1039/D1EN00763G).
- 105 R. M. Moshikur, I. M. Shimul, S. Uddin, R. Wakabayashi, M. Moniruzzaman and M. Goto, *ACS Appl. Mater. Interfaces*, 2022, **14**(50), 55332–55341, DOI: [10.1021/acsami.2c15636](https://doi.org/10.1021/acsami.2c15636).
- 106 C. G. Kolb, M. Lehmann, D. Kulmer and M. F. Zaeh, *Heliyon*, 2022, **8**, e11988, DOI: [10.1016/j.heliyon.2022.e11988](https://doi.org/10.1016/j.heliyon.2022.e11988).
- 107 D. Bitounis, H. Ali-Boucetta, B. H. Hong, D. H. Min and K. Kostarelos, *Adv. Mater.*, 2013, **25**, 2258–2268, DOI: [10.1002/adma.201203700](https://doi.org/10.1002/adma.201203700).
- 108 A. B. Saleem, R. Mamat, F. Y. Hagos, A. A. Abdullah and A. Arman, in *AIP Conf. Proc.*, 2022. DOI: [10.1063/5.0099886](https://doi.org/10.1063/5.0099886).
- 109 *Developing New Functional Food and Nutraceutical Products*, ed. S. Sen Gupta and M. Ghosh, Academic Press, 2016.
- 110 W. Ngo, S. Ahmed, C. Blackadar, B. Bussin, Q. Ji, S. M. Mladjenovic, Z. Sepahi and W. C. W. Chan, *Adv. Drug Delivery Rev.*, 2022, **185**, 114238, DOI: [10.1016/j.addr.2022.114238](https://doi.org/10.1016/j.addr.2022.114238).
- 111 K. Kozics, M. Sramkova, K. Kopecka, P. Begerova, A. Manova, Z. Krivosikova, Z. Sevcikova, A. Liskova, E. Rollerova, T. Dubaj, *et al.*, *Nanomaterials*, 2021, **11**, 1702, DOI: [10.3390/nano11071702](https://doi.org/10.3390/nano11071702).
- 112 B. Fadeel, C. Bussy, S. Merino, E. Vázquez, E. Flahaut, F. Mouchet, L. Evariste, L. Gauthier, A. J. Koivisto, U. Vogel, C. Martín, L. G. Delogu, T. Buerki-Thurnherr, P. Wick, D. Beloin-Saint-Pierre, R. Hischier, M. Pelin, F. C. Carniel, M. Tretiach, F. Cesca, F. Benfenati, D. Scaini, L. Ballerini, K. Kostarelos, M. Prato and A. Bianco, *ACS Nano*, 2018, **12**, 10582–10620, DOI: [10.1021/acs.nano.8b04758](https://doi.org/10.1021/acs.nano.8b04758).
- 113 L. Di Cristo, B. Grimaldi, T. Catelani, E. Vázquez, P. P. Pompa and S. Sabella, *Mater. Today Bio*, 2020, **6**, 100050, DOI: [10.1016/j.mtbio.2020.100050](https://doi.org/10.1016/j.mtbio.2020.100050).
- 114 S. P. Mukherjee, A. R. Gliga, B. Lazzaretto, B. Brandner, M. Fielden, C. Vogt, L. Newman, A. F. Rodrigues, W. Shao, P. M. Fournier, M. S. Toprak, A. Star, K. Kostarelos, K. Bhattacharya and B. Fadeel, *Nanoscale*, 2018, **10**, 1180–1188, DOI: [10.1039/c7nr03552g](https://doi.org/10.1039/c7nr03552g).
- 115 J. Zhang, Y. Yang, K. Li and J. Li, *J. Biomater. Sci., Polym. Ed.*, 2023, **34**(18), 2551–2576, DOI: [10.1080/09205063.2023.2265171](https://doi.org/10.1080/09205063.2023.2265171).
- 116 K. Yang, J. Wan, S. Zhang, Y. Zhang, S. T. Lee and Z. Liu, *ACS Nano*, 2011, **5**, 516–522, DOI: [10.1021/nn1024303](https://doi.org/10.1021/nn1024303).
- 117 G. Ban, Y. Hou, Z. Shen, J. Jia, L. Chai and C. Ma, *Int. J. Nanomed.*, 2023, **18**, 1695–1708, DOI: [10.2147/IJN.S402954](https://doi.org/10.2147/IJN.S402954).
- 118 P. A. Schulte and F. Salamanca-Buentello, *Environ. Health Perspect.*, 2007, **115**, 5–12, DOI: [10.1289/ehp.9456](https://doi.org/10.1289/ehp.9456).
- 119 A. Shafiee, S. Iravani and R. S. Varma, *MedComm*, 2022, **3**, e118, DOI: [10.1002/mco2.118](https://doi.org/10.1002/mco2.118).
- 120 F. Dormont, M. Rouquette, C. Mahatsekake, F. Gobeaux, A. Peramo, R. Brusini, S. Calet, F. Testard, S. Lepetre-Mouelhi, D. Desmaële and P. Couvreur, *J. Controlled Release*, 2019, **307**, 302–314, DOI: [10.1016/j.jconrel.2019.06.040](https://doi.org/10.1016/j.jconrel.2019.06.040).
- 121 G. Dong, Y. Hu, C. Guo, H. Wu, H. Liu, R. Peng, D. Xian, Q. Mao, Y. Dong, Y. Zhao, *et al.*, *Adv. Mater.*, 2022, **34**, e2108419, DOI: [10.1002/adma.202108419](https://doi.org/10.1002/adma.202108419).
- 122 J. Zhang, Q. Liu, Y. Ruan, S. Lin, K. Wang and H. Lu, *Chem. Mater.*, 2018, **30**, 1888–1897, DOI: [10.1021/acs.chemmater.7b04458](https://doi.org/10.1021/acs.chemmater.7b04458).
- 123 S. Yadav, *Pharma Innovation*, 2019, **8**, 870–874, DOI: [10.22271/tpi.2019.v8.i1n.25493](https://doi.org/10.22271/tpi.2019.v8.i1n.25493).
- 124 R. Vinayagam and V. P. Pande, *Int. J. ChemTech Res.*, 2015, **8**, 19–24.

